Postnatal maturation of GABAergic transmission in the rat basolateral amygdala

David E. Ehrlich, Steven J. Ryan, Rimi Hazra, Ji-Dong Guo and Donald G. Rainnie

J Neurophysiol 110:926-941, 2013. First published 29 May 2013; doi:10.1152/jn.01105.2012

J Neurophysiol 110: 926–941, 2013.
First published May 29, 2013; doi:10.1152/jn.01105.2012.

Postnatal maturation of GABAergic transmission in the rat basolateral amygdala

David E. Ehrlich, Steven J. Ryan, Rimi Hazra, Ji-Dong Guo, and Donald G. Rainnie
Department of Psychiatry and Behavioral Sciences, Emory University School of Medicine and Division of Behavioral Neuroscience and Psychiatric Disorders, Yerkes Research Center, Atlanta, Georgia

Submitted 28 December 2012; accepted in final form 28 May 2013

Ehrlich DE, Ryan SJ, Hazra R, Guo JD, Rainnie DG. Postnatal maturation of GABAergic transmission in the rat basolateral amygdala. *J Neurophysiol* 110: 926–941, 2013. First published May 29, 2013; doi:10.1152/jn.01105.2012.—Many psychiatric disorders, including anxiety and autism spectrum disorders, have early ages of onset and high incidence in juveniles. To better treat and prevent these disorders, it is important to first understand normal development of brain circuits that process emotion. Healthy and maladaptive emotional processing involve the basolateral amygdala (BLA), dysfunction of which has been implicated in numerous psychiatric disorders. Normal function of the adult BLA relies on a fine balance of glutamatergic excitation and GABAergic inhibition. Elsewhere in the brain GABAergic transmission changes throughout development, but little is known about the maturation of GABAergic transmission in the BLA. Here we used whole cell patch-clamp recording and single-cell RT-PCR to study GABAergic transmission in rat BLA principal neurons at postnatal day (P)7, P14, P21, P28, and P35. $GABA_A$ currents exhibited a significant twofold reduction in rise time and nearly 25% reduction in decay time constant between P7 and P28. This corresponded with a shift in expression of $GABA_A$ receptor subunit mRNA from the α2- to the α1-subunit. The reversal potential for $GABA_A$ receptors transitioned from depolarizing to hyperpolarizing with age, from around -55 mV at P7 to -70 mV by P21. There was a corresponding shift in expression of opposing chloride pumps that influence the reversal, from NKCC1 to KCC2. Finally, we observed short-term depression of $GABA_A$ postsynaptic currents in immature neurons that was significantly and gradually abolished by P28. These findings reveal that in the developing BLA GABAergic transmission is highly dynamic, reaching maturity at the end of the first postnatal month.

amygdala; $GABA_A$ receptor; development; chloride transporter; parvalbumin

THE AMYGDALA plays an important role in regulating emotional behaviors, particularly fear and anxiety (Davis et al. 2003; LeDoux 2007; Pape and Pare 2010). The basolateral nucleus of the amygdala (BLA), which, along with the lateral and accessory basal nuclei, comprises the basolateral complex of the amgydala, receives a large portion of the sensory input arriving in the amygdala (McDonald 1998). Dysfunction of the BLA has been implicated in the etiology of a variety of psychiatric disorders, including anxiety, depression, and autism spectrum disorders (Adolphs et al. 2002; Baron-Cohen et al. 2000; Neuhaus et al. 2010; Rainnie et al. 2004; Schumann et al. 2009; Shekhar et al. 2005; Sweeten et al. 2002; Truitt et al. 2007). These disorders are increasingly considered developmental in nature, highlighting a need for treatments targeted specifically to their pathogenesis in juveniles (Kim-Cohen et al. 2003; McEwen 2003; Pine et al. 1998; Steinberg 2005). Hence there is a critical need to characterize the developmental trajectory of the BLA and brain circuits that process emotion. Previously we have shown that the biophysical properties of neurons in the BLA change dramatically over the first postnatal month (Ehrlich et al. 2012). Here we focused on inhibitory synaptic transmission, which has been shown to be developmentally regulated (for reviews see Ben-Ari et al. 2012; Kilb 2012) and implicated in the pathophysiology of neurodevelopmental disorders (Chattopadhyaya and Cristo 2012; King et al. 2013).

Inhibitory synaptic transmission has been well characterized in the mature BLA (Martina et al. 2001; Rainnie et al. 1991; Washburn and Moises 1992), playing a fundamental role in determining the excitability of the region and thereby regulating emotional behavior (Ehrlich et al. 2009; Quirk and Gehlert 2003; Shekhar et al. 2003). Synaptic inhibition in the BLA is produced by intrinsic and extrinsic afferents activating local-circuit interneurons; these inhibitory neurons then release the neurotransmitter γ-aminobutyric acid (GABA) onto principal neurons, which comprise 80–85% of the BLA neuronal population (McDonald 1985, 1996). Blocking $GABA_A$ receptors in the BLA promotes fearful and anxious behaviors (for review see Quirk and Gehlert 2003), whereas enhancing GABA function attenuates these behaviors (Davis et al. 1994; Sanders and Shekhar 1995). GABAergic transmission in the BLA can also organize network activity; rhythmic inhibition of BLA principal neurons by burst-firing, parvalbumin-expressing interneurons can coordinate and synchronize firing of the principal neurons and may underlie network oscillations in the BLA related to fear (Ryan et al. 2012).

In addition to regulating neuronal activity in the adult brain, $GABA_A$ receptors undergo functional maturation and serve to coordinate brain development. One well-established trigger for the onset of "critical periods," or developmental windows of high plasticity, is activity at $GABA_A$ receptors (Hensch 2005). This action depends on the subunit composition of $GABA_A$ receptors, which are comprised of five subunits and typically contain two α-, two β-, and one γ-subunit. There are six known α-subunits, and the relative expression of these subunits changes throughout development. The α-subunits influence the kinetics, localization, and drug sensitivity of $GABA_A$ receptors (Hevers and Luddens 2002; Nusser et al. 1996). As the brain develops, expression shifts from high levels of the α2-subunit toward the α1-subunit, which confers faster kinetics (Bosman et al. 2002; Davis et al. 2000; Dunning et al. 1999; Eyre et al. 2012; Hornung and Fritschy 1996; Mohler et al. 2004).

Address for reprint requests and other correspondence: Donald G. Rainnie, Emory Univ. School of Medicine, Dept. of Psychiatry and Behavioral Sciences, Div. of Behavioral Neuroscience and Psychiatric Disorders, Yerkes Research Center, Atlanta, GA 30329 (e-mail: drainni@emory.edu).

$GABA_A$ receptor function in the brain changes in another fundamental way, switching from excitatory at birth to inhibitory in adulthood (for review see Ben-Ari et al. 2012). This switch is believed to result from developmental changes to the concentration gradient of chloride, the ion mediating $GABA_A$ currents. At birth, there is greater expression of sodium-potassium-chloride cotransporter 1 (NKCC1), which accumulates intracellular chloride and renders $GABA_A$ receptors excitatory. In adulthood, potassium-chloride cotransporter 2 (KCC2) is expressed more highly, extruding chloride from the cell and rendering $GABA_A$ receptors inhibitory (Ben-Ari et al. 2012). Excitatory GABA early in development is thought to promote calcium influx and modulate neuronal growth and synapse formation (Ben-Ari et al. 1997).

Aside from the precedent for GABAergic maturation observed elsewhere in the brain, there are good reasons to expect that similar changes occur in the developing BLA. For example, we recently showed that the electrophysiological properties of BLA principal neurons mature rapidly from postnatal day (P)7 to P21, including a 10-fold reduction in input resistance and a 3-fold reduction in membrane time constant, suggesting that the sensitivity to synaptic inhibition would also vary greatly (Ehrlich et al. 2012). There are also concurrent changes in the expression and connectivity of GABAergic interneurons in the BLA, including the emergence and maturation of parvalbumin-expressing interneurons between P14 and P30 (Berdel and Moryś 2000; Davila et al. 2008). Between P14 and P20, there is a significant increase in the density of GABAergic fibers and a decrease in the density of GABAergic cell bodies in the BLA (Brummelte et al. 2007). Further evidence comes from the development of behaviors related to BLA function. There is a switch from paradoxical approach to an aversively conditioned stimulus to the mature, avoidance behavior at P10, corresponding with a change in synaptic plasticity that is reversed by $GABA_A$ blockade (Sullivan et al. 2000; Thompson et al. 2008). In addition, rats exhibit suppression of fear learned at P18 but not P23, a phenomenon called infantile amnesia that is $GABA_A$ receptor dependent (Kim et al. 2006). The mechanisms of fear extinction also change in this window, becoming amygdala- and GABA dependent between P17 and P24 (Kim and Richardson 2008). There are several additional examples of rapid, developmental changes to the expression and underlying physiology of fear learning (Campbell and Ampuero 1985; Hunt et al. 1994; Moye and Rudy 1987; Tang et al. 2007).

Despite the variety of documented changes to the BLA circuit and emotional behavior across the first postnatal month, and the critical role that synaptic inhibition plays in the function of the adult amygdala, no study to date has examined the developmental profile of GABAergic transmission in the immature BLA. To address this knowledge gap, we have used a combination of patch-clamp electrophysiology and single-cell reverse transcription-polymerase chain reaction (RT-PCR) to characterize the properties of synaptic inhibition of BLA principal neurons across the first postnatal month. Here we outline significant changes in terms of the kinetics, reversal potential, and short-term synaptic plasticity (STP) of $GABA_A$ receptor activation as well as underlying changes in gene expression. In this study we characterized normative amygdala development to enable future studies to address the contribution of the amygdala to both healthy and maladaptive emotional development.

MATERIALS AND METHODS

Ethical approval. All experimental protocols strictly conform to the National Institutes of Health *Guide for the Care and Use of Laboratory Animals* and were approved by the Institutional Animal Care and Use Committee of Emory University.

Animals. Rats born in-house to time-mated female Sprague-Dawley rats (Charles River, Wilmington, MA) were used in all experiments. Pups were housed with the dam prior to weaning on P22 or P23 (considering P1 as day of birth). After weaning, rats were isolated by sex and housed three to four per cage with access to food and water ad libitum. Animals were killed for electrophysiological recordings at P7–10, P13–15, P20–22, P27–29, and P33–36, and for brevity these windows are described as single time points. To maximize the use of animals, experiments on $GABA_A$ reversal and for single-cell RT-PCR included data from the offspring of dams used as negative control subjects for other studies. In these cases, data were grouped because there was no observable difference in standard-raised animals and those born from dams receiving either manipulation.

Slice preparation. Slices containing the BLA were obtained as previously described (Rainnie 1999). Briefly, animals were decapitated under isoflurane anesthesia (Fisher Scientific, Hanover Park, IL) if older than P11, and the brains were rapidly removed and immersed in ice-cold 95% oxygen-5% carbon dioxide-perfused "cutting solution" with the following composition (in mM): 130 NaCl, 30 $NaHCO_3$, 3.50 KCl, 1.10 KH_2PO_4, 6.0 $MgCl_2$, 1.0 $CaCl_2$, 10 glucose, 0.4 ascorbate, 0.8 thiourea, 2.0 sodium pyruvate, and 2.0 kynurenic acid. Coronal slices containing the BLA were cut at a thickness of 300–350 μm with a Leica VTS-1000 vibrating blade microtome (Leica Microsystems, Bannockburn, IL). Slices were kept in oxygenated cutting solution at 32°C for 1 h before transfer to regular artificial cerebrospinal fluid (ACSF) containing (in mM) 130 NaCl, 30 $NaHCO_3$, 3.50 KCl, 1.10 KH_2PO_4, 1.30 $MgCl_2$, 2.50 $CaCl_2$, 10 glucose, 0.4 ascorbate, 0.8 thiourea, and 2.0 sodium pyruvate.

Whole cell patch clamp. Individual slices were transferred to a recording chamber mounted on the fixed stage of a Leica DMLFS microscope (Leica Microsystems) and maintained fully submerged and continuously perfused with oxygenated 32°C ACSF at a flow rate of 1–2 ml/min. The BLA was identified under ×10 magnification. Individual BLA neurons were identified at ×40 with differential interference contrast optics and infrared illumination with an infrared-sensitive CCD camera (Orca ER, Hamamatsu, Tokyo, Japan). Patch pipettes were pulled from borosilicate glass and had a resistance of 4–6 MΩ. We used two patch electrode solutions, one based on potassium gluconate for current-clamp recordings and one based on cesium gluconate for voltage-clamp recordings. The potassium gluconate patch solution had the following composition (in mM): 140 potassium gluconate, 2 KCl, 10 HEPES, 3 $MgCl_2$, 2 K-ATP, 0.2 Na-GTP, and 5 phosphocreatine, was titrated to pH 7.3 with KOH, and was 290 mosM. The cesium gluconate patch solution had the following composition (in mM): 131 CsOH, 131 gluconate, 10 HEPES, 2 $CaCl_2$, 10 glucose, 10 EGTA, 5 Mg-ATP, and 0.4 Na-GTP, was titrated to pH 7.3 with gluconate, and was 270 mosM. To visualize the recording sites of some neurons, 0.35% biocytin (Sigma-Aldrich, St. Louis, MO) was added to the patch solution and tissue was stained as previously described (Rainnie et al. 2006) and imaged at ×5 magnification on a Leica DM5500B microscope (Leica Microsystems) equipped with a CSU10B Spinning Disk (Yokagawa Electronic, Tokyo, Japan).

Data acquisition was performed with a MultiClamp 700A or Axopatch 1D amplifier in conjunction with pCLAMP 10.2 software and a DigiData 1322A AD/DA interface (Molecular Devices, Sunnyvale, CA). Whole cell patch-clamp recordings were obtained, low-pass filtered at 2 kHz, and digitized at 10 kHz. Cells were excluded if

they did not meet the following criteria: a resting membrane potential more negative than −55 mV and drifting <5 mV over the course of the recording session; access resistance lower than 30 MΩ; stable access resistance throughout recording, changing <15%; and action potentials crossing 0 mV. Recordings were only included from BLA principal neurons, which can be distinguished from BLA interneurons for electrophysiological recordings by a combination of their large somatic volume, low input resistance, slow action potentials, and relatively low synaptic input (Rainnie et al. 1993). Furthermore, we previously reported that 58 of 60 putative principal neurons recorded in the immature BLA were found positive for mRNA for the vesicular glutamate transporter by single-cell RT-PCR (Ehrlich et al. 2012).

Spontaneous inhibitory postsynaptic currents. To quantify changes in the kinetics of $GABA_A$ inhibitory postsynaptic currents (IPSCs) in developing BLA principal neurons, spontaneous IPSCs were measured from 30-s-long recordings in voltage-clamp mode with a cesium gluconate-based patch solution. Outward synaptic currents were measured at −50 mV, unless discernible outward currents were observed at −60 mV. Neurons were only included in this analysis if their outward synaptic currents exhibited a reversal potential below −50 mV. Synaptic currents were selected by hand by a blinded experimenter from traces low-pass filtered at 500 Hz, and kinetics were analyzed off-line with Mini Analysis 6.0.3 (Synaptosoft, Decatur, GA). Event detection parameters were as follows: time before a peak for baseline (7.5 ms), period to search a decay time (50 ms), fraction of peak to find a decay time (0.368), and period to average a baseline (5 ms). Ten to ninety percent rise time and decay time constant were measured automatically based on the detected baseline and peak, using the time to reach 0.1 and 0.9 of the peak on the rising phase and 0.368 of the peak on the falling phase. An individual IPSC was excluded from analysis if its detected rise time was longer than its decay time, and a neuron was excluded if it had fewer than five IPSCs for analysis. For illustration, IPSC waveforms were temporally aligned by rise time in MiniAnalysis and then smoothed with a sliding window of 2-ms width and averaged with MATLAB (The MathWorks, Natick, MA).

Stimulation-evoked postsynaptic potentials and currents. To measure the duration of the network response and the reversal potential and STP of $GABA_A$ receptor-mediated events in BLA principal neurons, a bipolar stimulating electrode was placed in the dorsal end of the BLA, just medial to the external capsule (Fig. 1). The initial, half-maximal response was recorded in current clamp when using potassium-based patch solution and voltage clamp when using cesium-based patch solution. Durations of the voltage-clamp responses were measured with Clampfit 10.2 (Molecular Devices) by an experimenter blind to postnatal age, from the stimulation artifact to the return to resting membrane potential, and the duration was averaged for the responses at −50, −60, and −70 mV.

To isolate from the initial response monosynaptic $GABA_A$ postsynaptic currents (PSCs) and potentials (PSPs), stimulation at 0.2 Hz was applied after application of a cocktail of synaptic blockers, including the AMPA/kainate receptor antagonist 6,7-dinitroquinoxaline-2,3-dione (DNQX, 20 μM; Sigma-Aldrich), the NMDA receptor antagonist 3-(2-carboxypiperazin-4-yl)propyl-1-phosphonic acid (RS-CPP, 10 μM; Tocris Bioscience, Bristol, UK), and the $GABA_B$ receptor antagonist (2*S*)-3-[[(1*S*)-1-(3,4-dichlorophenyl)ethyl]amino-2-hydroxypropyl] (phenylmethyl)phosphinic acid hydrochloride (CGP52432, 2 μM; Tocris). Placement of the stimulating electrode medial to the external capsule was often required to elicit a response in the presence of glutamatergic synaptic blockers. Stimulation intensity was adjusted to elicit a half-maximal response after application of blockers. To verify that the isolated response was purely $GABA_A$, some experiments culminated with the application of the $GABA_A$ antagonist 6-imino-3-(4-methoxyphenyl)-1(6*H*)-pyridazinebutanoic acid hydrobromide (SR95531, 5 μM; Tocris). Reversal potential was estimated from $GABA_A$ PSPs evoked in neurons at least 15 min after patching with the potassium gluconate-based solution. Reversal potential was interpolated from stimulation responses in neurons adjusted with direct current injection to baseline recording potentials spanning the reversal, including three of the following: approximately −50, −60, −70, and −80 mV. The average response of five sweeps at each baseline potential was used for calculation with Clampfit.

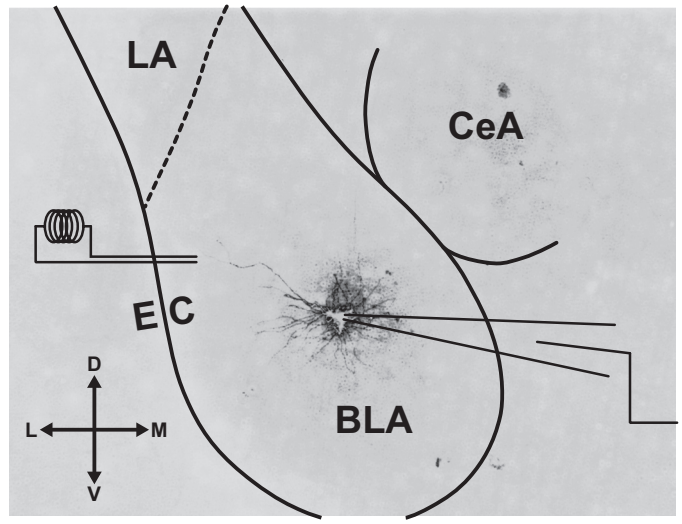

Fig. 1. Schematic of recording and stimulation sites. Photomicrograph of a coronal slice of medial temporal lobe, depicting a representative, filled basolateral amygdala (BLA) principal neuron at postnatal day (P)14 in the target recording site. The bipolar stimulating electrode was placed medial to the external capsule (EC) within the BLA. The lateral nucleus (LA) and central nucleus (CeA) of the amygdala are also labeled. The compass gives directions for dorsal (D), ventral (V), lateral (L), and medial (M).

To analyze STP of $GABA_A$ PSCs neurons were voltage-clamped at −50 or −60 mV, and only outward currents were used. Trains of five pulses at 10 and 20 Hz were evoked for each neuron, and five sweeps were presented at 0.1 Hz. The sweeps were averaged in Clampfit, and amplitudes were measured for each pulse from the 1 ms prior to the stimulation artifact to the absolute peak deflection. The ratios of the amplitudes of *pulse 2* and *pulse 5* to *pulse 1* were calculated at both frequencies and used for statistical analyses.

Picospritzer response. The exogenous $GABA_A$ receptor agonist muscimol (Sigma-Aldrich) was focally applied to patch-clamped neurons with a picospritzer (Parker Hannifin, Cleveland, OH). After patching, the tip of a second pipette, identical to microelectrodes for patch clamping and filled with a solution of 100 μM muscimol dissolved in regular ACSF, was brought within 15 μm of the soma of the patched neuron. Five responses (0.1 Hz) to 5-ms puffs of muscimol at 5 PSI were recorded in voltage clamp at −50, −60, and −70 mV. The majority of responses were measured in the presence of bath-applied tetrodotoxin (TTX, 1 μM; Tocris), but there was no discernible difference with or without the drug, so data were pooled. Decay time constant was measured from the average response with a single-exponential fit in Clampfit. The reversal potential of the picospritzer response was estimated from the peak of the mean response at each recording voltage by interpolation. The peak conductance was calculated for, and averaged across, the response at each voltage, excluding any recordings made within 5 mV of the estimated reversal potential.

Single-cell and whole tissue RT-PCR. To perform single-cell RT-PCR, at the end of the patch-clamp recording session the cell cytoplasm was aspirated into the patch recording pipette by applying gentle negative pressure under visual control. Pipettes contained ~5 μl of RNase-free patch solution. The contents of the patch pipette were expelled into a microcentrifuge tube containing 5 μl of the reverse transcription cocktail (Applied Biosystems, Foster City, CA). The reverse transcription product was amplified in triplicate and

screened for 18S rRNA. Only those cell samples positive for 18S rRNA were subjected to amplification with primers. The procedure used to determine mRNA transcript expression in single cells has been described in detail previously (Hazra et al. 2011). The sequences for the oligonucleotide primers are detailed in Table 1. PCR products were visualized by staining with ethidium bromide and separated by electrophoresis in a 1% agarose gel. RT-PCR was also performed on whole BLA of P7 rats, from tissue isolated by microdissection from 300-μm-thick slices. The slices were made with the protocol for electrophysiological recording described above, and RNA isolation and RT-PCR were performed as described previously (Hazra et al. 2011).

Statistics. All statistical analyses were performed with Prism 4 (GraphPad, LaJolla, CA). All tests for significant effects of age were performed with one-way ANOVAs, except for the effects of age on STP, which was tested with a two-way ANOVA with repeated measures, with the second factor being stimulation frequency. For all ANOVAs and posttests, significance was defined at $\alpha = 0.05$. To perform pairwise comparisons following significant main effects in ANOVA, Tukey's posttests were generally used. The only exception was the two-way ANOVA, which was followed by Bonferroni posttests comparing all pairs of group means. For the estimation of $GABA_A$ reversal potential, one data point in the P7 group was more than 2 standard deviations from the group mean and was therefore excluded from analysis. To perform a one-way ANOVA on the peak conductance of IPSCs, data were log-transformed to correct for heteroscedasticity assessed with Bartlett's test.

RESULTS

Compound synaptic response to local electrical stimulation. In total, we made whole cell patch-clamp recordings from 170 BLA principal neurons from 62 rats of ages ranging from P7 to P36. We first investigated whether the response of the local BLA network to electrical stimulation changed during the first postnatal month (Fig. 2). Here, we characterized the stimulation response in current clamp at three different baseline membrane potentials and found three distinct components (Fig. 2*A*). The first, a fast excitatory component, was depolarizing at all ages and was blocked by the AMPA/kainate receptor antagonist DNQX (20 μM, data not shown). There was also a fast inhibitory response (Fig. 2*A*, filled arrowheads) that shunted the glutamatergic component at all ages and was blocked by the specific $GABA_A$ receptor antagonist SR95531 (5 μM, data not shown). Finally, there was a second, slower inhibitory component (Fig. 2*A*, open arrowheads) that was blocked by the specific $GABA_B$ receptor antagonist CGP52432 (2 μM, data not shown). With age, there was an apparent hyperpolarization of the reversal potential of the $GABA_A$ component and an apparent reduction of the amplitude and duration of the $GABA_B$ response. In P7 neurons, the stimulation response had a long duration, typically lasting >1 s ($n = 18$). By P14, the $GABA_B$ component generally had smaller amplitude and duration, lasting <1 s ($n = 17$). Responses were highly similar between P21 and P28, with a fast, inhibitory $GABA_A$ peak and a $GABA_B$ response that terminated within 500 ms of stimulation ($n = 11$ for P21, 8 for P28).

Between P7 and P28 the input resistance and membrane time constant of BLA principal neurons show 10- and 3-fold reduction, respectively (Ehrlich et al. 2012), which would dramatically alter the waveform of the evoked PSPs. Hence we next

Table 1. *PCR primers used in this study*

Gene	Accession No.	Primer Sequence	PCR Product Size, bp
18S rRNA	X01117	F: 5′-CCGGCGGCTTTGGTGACTCTA-3′ R: 5′-GCTCGGGCCTGCTTTGAACA-3′	563
GABAα1	AY574250	F: 5′-TGCCCATGCCTGCCCACTAAAA-3′ R: 5′-GCCATCCCACGCATACCCTCTCT-3′	511
GABAα2	P23576	F: 5′-CCA GTC AAT TGG GAA GGA GAC AAT-3′ R: 5′-TAG GCG TTG TTC TGT ATC ATG ACG-3′	434
GABAα3	X51991	F: 5′-T GTT GTT GGG ACA GAG ATA ATC CG-3′ R: 5′-CAC TGT TGG AGT TGA AGA AGC ACT-3′	549
GABAα4	P28471	F: 5′-AGC TGC CCC AGT ACT GAA GGA AAA-3′ R: 5′-ACT GTT GTC TTA ATG CGC CCA AGT-3′	374
GABAα5	X51992	F: 5′-ACA GTA GGC ACT GAG AAC ATC AGC-3′ R: 5′-AGG ATG GGT CAA CTT CCC AGT TGT-3′	407
GABAα6	NM_021841	F: 5′-CAAGCTCAACTTGAAGATGAAGG-3′ R: 5′-TCCATCCATAGGGAAGTTAACC-3′	416
GABAβ1	NM_012956	F: 5′-ACAGCTCCAATGAACCCAGCAA-3′ R: 5′-TGCTCCCTCTCCTCCATTCCA-3′	521
GABAβ2	X15467	F: 5′-GGAGTGACAAAGATTGAGCTTCCT-3′ R: 5′-GTCTCCAAGTCCCATTACTGCTTC-3′	564
GABAβ3	NM_017065	F: 5′-CCGTCTGGTCTCCAGGAATGTTGTC-3′ R: 5′-CGATCATTCTTGGCCTTGGCTGT-3′	411
GABAγ1	NM_080586	F: 5′-CAATAAAGGAAAAACCACCAG-3′ R: 5′-TGATTATATTGGACTAAGCCAGA-3′	374
GABAγ2	L08497	F: 5′-GTGAAGACAACTTCTGGTGACTATGTGGT-3′ R: 5′-CATATTCTTCATCCCTCTCTTGAAGGTG-3′	415
GABAγ3	X63324	F: 5′-CTGCTGCTTCTCCTCTGCCTGTTC-3′ R: 5′-GGTTGGGTGTGGTGATCCAGTGA-3′	423
GABAδ	NM_017289	F: 5′-AGCAGTGCCTGCCAGAGTAT-3′ R: 5′-CATGTAAAGCCGTCATGTGG-3′	563
KCC2	NM_134363.1	F: 5′-AGGTGGAAGTCGTGGAGATG-3′ R: 5′-CGAGTGTTGGCTGGATTCTT-3′	190
NKCC1	NM_031798.1	F: 5′-CCTGATCTCTGCGGGTATCTTT-3′ R: 5′-ACCTTTCGCAAACATCTGGAA-3′	130

F, forward; R, reverse.

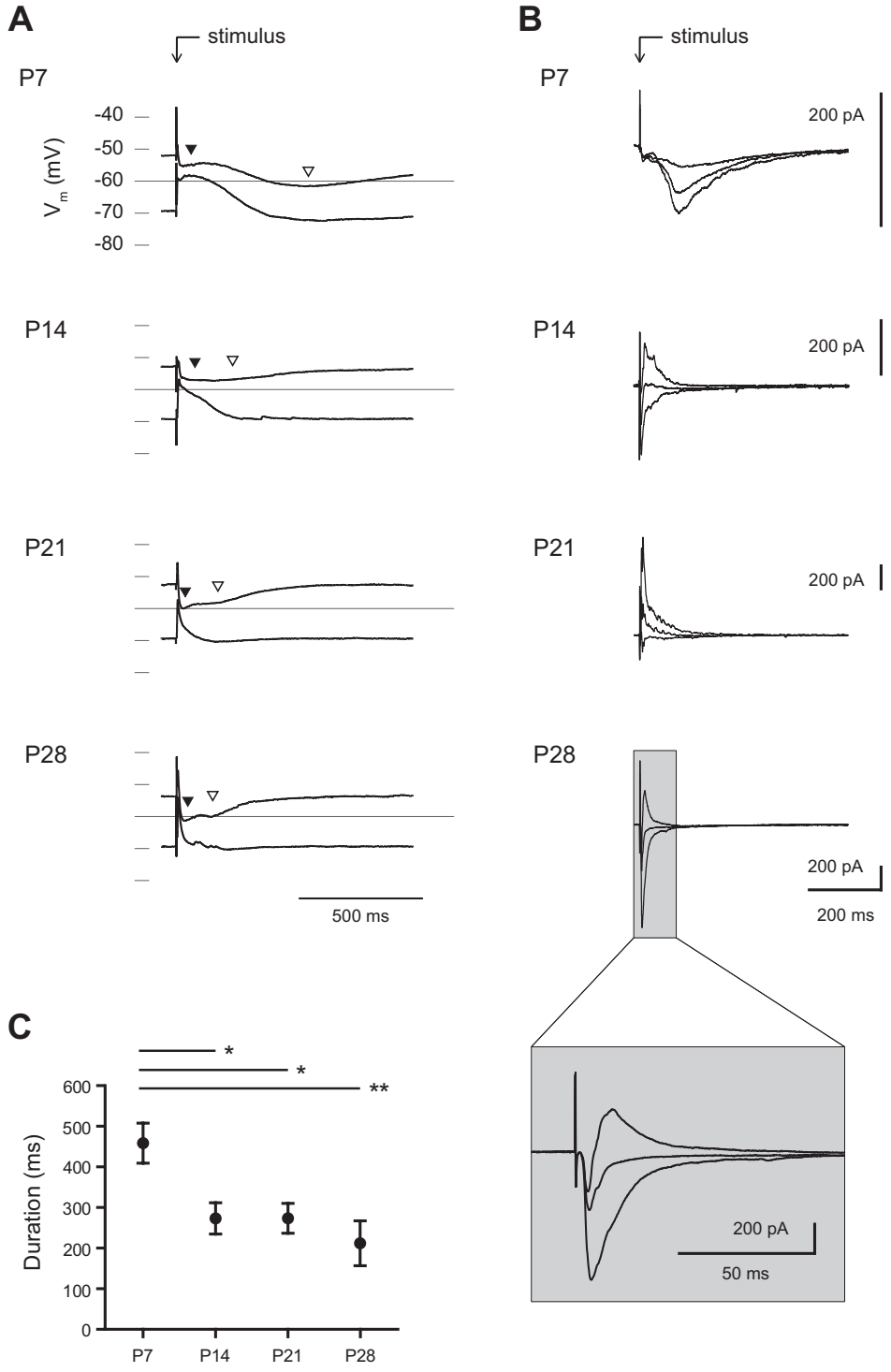

Fig. 2. Maturation of the stimulation response within the BLA. *A* and *B*: the average waveform of the response to 5 stimulations (0.1 Hz) of the dorsolateral BLA is shown for representative neurons at P7, P14, P21, and P28 from recordings in current clamp (*A*) and voltage clamp (*B*). Neurons in current clamp were adjusted before stimulation to a baseline membrane potential (V_m) of approximately −50 or −70 mV, and the responses are plotted on single voltage axes. Highlighted on the plots are the $GABA_A$ (filled arrowheads) and $GABA_B$ (open arrowheads) components of the response. Neurons in voltage clamp were recorded from holding potentials of −50, −60, and −70 mV, and baselines were subtracted for comparison. The $GABA_B$ component was blocked in the voltage-clamp recordings to highlight the $GABA_A$ response. *C*: the duration of the stimulation response in voltage clamp is plotted for each time point as mean ± SE. Significance was assessed with a 1-way ANOVA ($F_{3,60} = 5.807$, $P < 0.001$) and Tukey's posttests [$^*P < 0.05$, $^{**}P < 0.01$, $n = 18$ (P7), 17 (P14), 18 (P21), 11 (P28)].

measured the properties of evoked synaptic currents in voltage-clamp mode in another set of neurons. By blocking the $GABA_B$ component with a cesium-based patch solution, we were able to isolate the $GABA_A$ component of the evoked response (Fig. 2*B*). Consistent with our current-clamp recordings, stimulation at holding potentials of −50, −60, and −70 mV reliably resulted in a fast excitatory PSC (EPSC) at every time point examined and a $GABA_A$ PSC that became faster with age. We measured the duration of the $GABA_A$ response, which exhibited a significant, threefold reduction across the first postnatal month (Fig. 2*C*; 1-way ANOVA, $F_{3,60} = 5.81$, $P < 0.001$). A majority of the change occurred between P7 and P14, with a significant reduction in duration (mean ± SE) from 466.0 ± 49.1 ms at P7 ($n = 18$) to 280.9 ± 38.4 ms at P14 ($n = 17$; Tukey's posttest, $P < 0.01$). The duration was relatively stable from P14 to P21 and P28, with a value of 281.0 ± 36.6 ms at P21 ($n = 18$) and 219.6 ± 55.1 ms at P28 ($n = 11$). The stimulation response at P28 matched the biphasic response seen in adult BLA principal neurons, with a fast glutamatergic EPSC that is rapidly shunted by a GABAergic

IPSC (see Fig. 2*B*, *inset*). We hypothesized that the slow $GABA_A$ response in immature BLA neurons was due to slow individual $GABA_A$ PSCs or, alternatively, to the depolarized reversal potential of $GABA_A$ receptors removing a brake on network activity. Therefore, we next quantified the kinetics and reversal potential of isolated $GABA_A$ receptor-mediated currents in BLA principal neurons across the first postnatal month.

Kinetics of fast synaptic inhibition of BLA principal neurons. To quantify changes to the kinetics of $GABA_A$ currents in BLA principal neurons we recorded spontaneous IPSCs (Fig. 3). Across the first postnatal month, IPSCs became significantly faster with age until around P21 (Fig. 3*A*). In particular, IPSC 10–90% rise time exhibited a significant decrease of more than twofold across the first postnatal month (Fig. 3*B*; 1-way ANOVA, $F_{3,36} = 7.80$, $P < 0.001$). There was also a significant reduction across this window in the time constant of IPSC decay (Fig. 3*C*; 1-way ANOVA, $F_{3,36} = 3.45$, $P < 0.05$) and a similar trend in IPSC half-width (Fig. 3*D*). Specifically, spontaneous IPSCs of neurons at P7 were relatively slow, with a rise time (mean ± SE) of 2.29 ± 0.34 ms, a decay time constant of 5.76 ± 0.19 ms, and a half-width of 5.86 ± 0.59 ms ($n = 6$). By P14 rise time was reduced to 1.68 ± 0.14 ms, although decay time constant and half-width were relatively unchanged at 6.13 ± 0.43 ms and 5.70 ± 0.40 ms, respectively ($n = 16$). At P21 IPSCs were faster, with rise time reduced to 1.15 ± 0.12 ms, decay time constant reduced to 4.93 ± 0.22 ms, and half-width reduced to 4.65 ± 0.19 ms ($n = 11$). At P28 IPSCs showed kinetics similar to those at P21 and were significantly faster than at younger ages; rise time was 1.10 ± 0.12 ms (Tukey's posttests, $P < 0.001$ vs. P7 and $P < 0.01$ vs. P14), decay time constant was 4.59 ± 0.36 ms ($P < 0.05$ vs. P14), and half-width was 4.51 ± 0.42 ms (not significant; $n = 7$).

Unlike IPSC kinetics, there was no age-dependent change in the size of spontaneous IPSCs. We found no significant effect of age on peak conductance, although it tended to increase with age (Fig. 3*E*; 1-way ANOVA, $F_{3,23} = 0.87$, $P > 0.05$; $n = 5$ or 6). At later time points there was an emergence of large IPSCs not observed at P7, but they were not frequent enough to significantly alter the mean conductance. Moreover, no significant difference was observed in the coefficient of variation of peak conductance for each neuron with age (Fig. 3*F*; $F_{3,22} = 1.28$, $P > 0.05$; $n = 5$ or 6). There was a weak positive correlation of peak IPSC conductance and decay time constant ($R^2 < 0.2$ at each age; data not shown).

To exclude the possibility that the developmental change in IPSC kinetics was due to presynaptic effects, we also measured responses to focal application of the $GABA_A$ receptor agonist muscimol (Fig. 4). As illustrated in Fig. 4*A*, the tip of a pipette was placed near a patched BLA principal neuron, and 100 μM muscimol was picospritzed onto the soma. The muscimol response became much larger and faster with age, as seen in Fig. 4, *B* and *C*. There was a significant overall effect of age on the decay time constant of the response, with a significant decrease between P14 and P21 (Fig. 4*D*; 1-way ANOVA with Tukey's posttests, $F_{3,53} = 5.57$, $P < 0.01$). At P7, the decay time constant of the muscimol response was 407.7 ± 54.2 ms (mean ± SE, $n = 12$), which increased to 431.1 ± 34.7 ms at P14 ($n = 16$). The decay time constant then decreased signif-

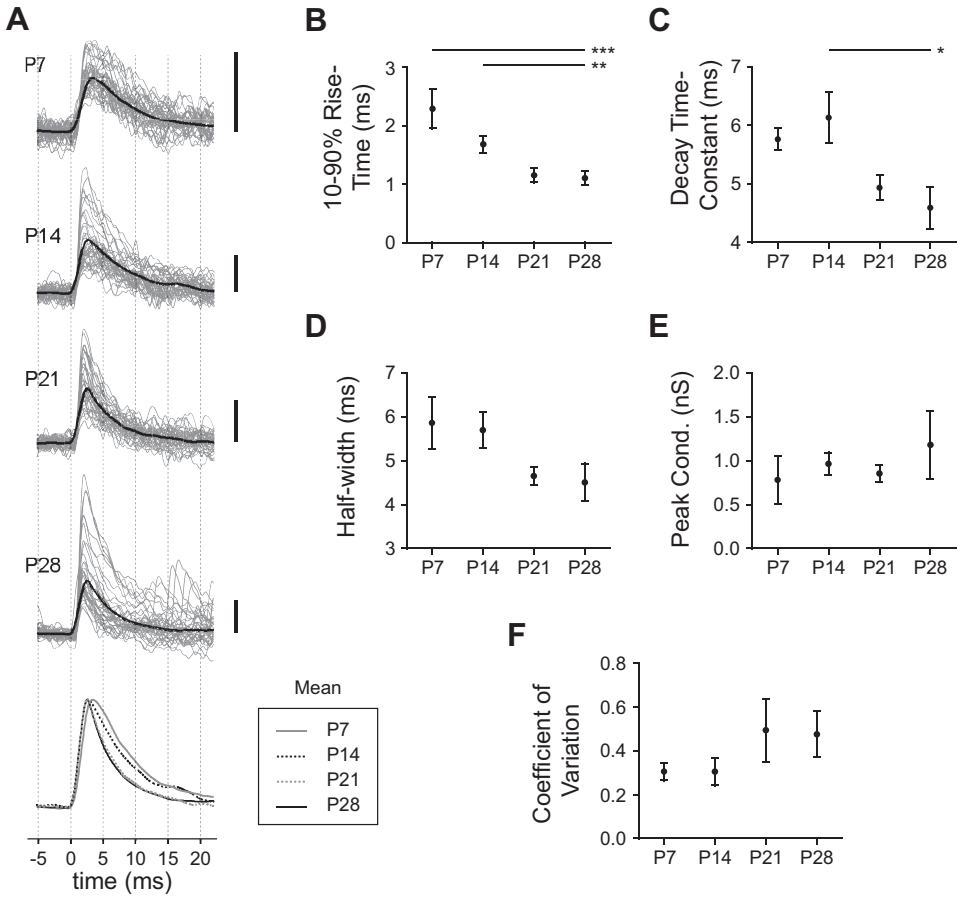

Fig. 3. Development of spontaneous inhibitory postsynaptic current (IPSC) kinetics across the first postnatal month. *A*: the waveforms of spontaneous IPSCs are illustrated for representative neurons at P7, P14, P21, and P28, depicted as the mean (black line) of all IPSCs recorded in a 30-s window as well as the first 40 IPSCs observed in these windows (gray lines). Scale bars, 10 pA. Mean waveforms are superimposed (*bottom*) for comparison. *B–F*: at each time point, mean ± SE is plotted for IPSC 10–90% rise time (*B*), decay time constant (*C*), half-width (*D*), and peak conductance (*E*) as well as the coefficient of variation of the peak conductance for each neuron (*F*). Significance was assessed with 1-way ANOVAs and Tukey's posttests (*$P <$ 0.05, **$P < 0.01$, ***$P < 0.001$), identifying a significant main effect of age on IPSC rise time ($F_{3,36} = 7.80$, $P < 0.001$) and decay time constant ($F_{3,36} = 3.45$, $P < 0.05$) but not half-width [$n = 6$ (P7), 16 (P14), 11 (P21), 7 (P28)]. No significant effect of age was detected for peak conductance ($F_{3,23} = 0.87$, $P > 0.05$) or coefficient of variation ($F_{3,22} = 1.28$, $P > 0.05$; $n = 5$ or 6).

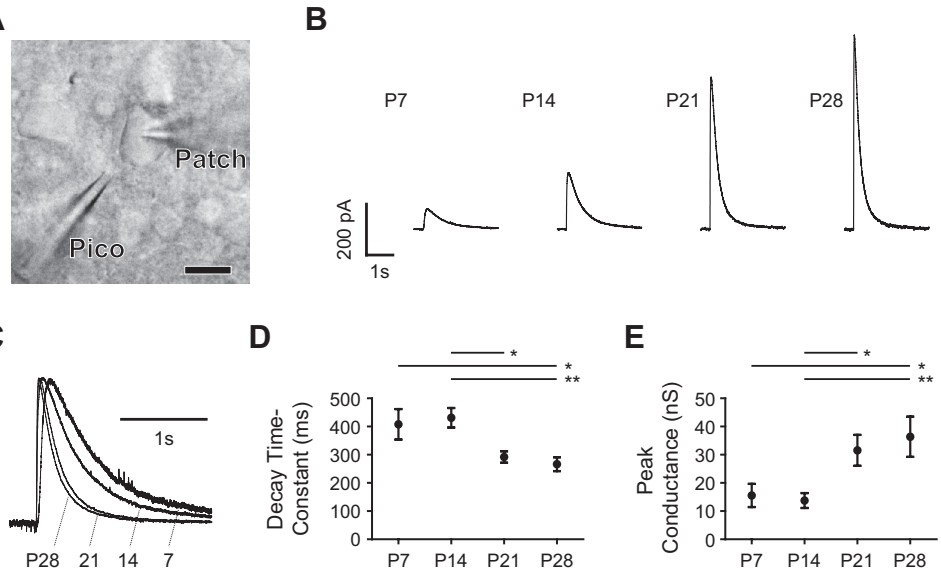

Fig. 4. Maturation of the response to exogenous $GABA_A$ agonist. *A*: BLA principal neurons at P7, P14, P21, and P28 were patch-clamped with a patch electrode (Patch), and a microelectrode containing 100 μM muscimol (Pico) was brought in close proximity to the soma. Scale bar, 10 μm. *B*: mean responses in voltage clamp at -50 mV to picospritzer application of muscimol in a representative neuron at each time point. *C*: responses from *B* are normalized and superimposed to highlight decay kinetics. *D* and *E*: the decay time constant (*D*) and peak conductance (*E*) of the muscimol response are plotted as mean ± SE for each time point. Significance was assessed with 1-way ANOVAs and Tukey's posttests (*$P < 0.05$, **$P < 0.01$), identifying a significant main effect of age on decay time constant [$F_{3,53} = 5.57$, $P < 0.01$; $n = 12$ (P7), 16 (P14), 13 (P21), 13 (P28)] and peak conductance [$F_{3,43} = 5.67$, $P < 0.01$; $n = 10$ (P7), 14 (P14), 10 (P21), 10 (P28)].

icantly to 291.9 ± 20.3 ms at P21 ($P < 0.05$; $n = 12$) and 266.3 ± 24.6 ms at P28 ($P < 0.01$; $n = 12$). The inverse developmental trajectory was observed for the peak conductance of the muscimol response, which increased significantly with age and also transitioned abruptly from P14 to P21 (Fig. 4*E*; 1-way ANOVA with Tukey's posttests, $F_{3,43} = 5.67$, $P < 0.01$). At P7 the peak conductance was 15.6 ± 4.1 nS ($n = 10$), which decreased to 13.8 ± 2.6 nS at P14 ($n = 14$). The peak conductance then increased significantly to 31.6 ± 5.5 nS at P21 ($P < 0.05$; $n = 10$) and 36.4 ± 7.1 nS at P28 ($P < 0.01$; $n = 10$).

The kinetics of $GABA_A$ receptors are influenced by their subunit composition, which is classically regulated during development. Hence we next used single-cell RT-PCR to identify developmental changes in the expression of $GABA_A$ receptor subunit mRNA in BLA principal neurons (Fig. 5). There was an age-dependent increase in the proportion of neurons with detectable transcripts for 7 of the 13 $GABA_A$ receptor subunits tested: namely, α1, α2, α3 and α5, β2 and β3, and γ2 (Fig. 5, *A* and *B*; $n = 10$). No expression was detected for α4, α6, β1, γ3, or δ, and only one neuron at any age was found to express γ1 mRNA. There was no detectable expression of any subunit transcripts at P7; however, because rRNA for the housekeeper gene 18S was present in all cells used for this analysis, we assume this was due to limited sensitivity of the technique for low levels of transcript. As a positive control, we screened whole BLA tissue for mRNA of $GABA_A$ receptor subunits (Fig. 5*C*); as early as P7, the whole BLA contained detectable levels of mRNA for every subunit screened ($n = 4$).

Using single-cell RT PCR, we observed an increase in the expression of the α1 subunit, which confers faster IPSC kinetics, relative to that of α2, which confers slower IPSC kinetics. Specifically, while 4 of 10 neurons at P14 expressed α2 mRNA, 0 had expression for α1; by P28 the proportions for the subunits were comparable, with 4 and 6 of 10 neurons expressing α1 and α2, respectively. Interestingly, there was a strong clustering effect at P21 and P28, with the β3 subunit being expressed by 11 of 12 neurons with detectable expression of α2 but 0 of 7 with α1. The β2- and γ2-subunits had the opposite pattern: β2 and γ2 were detected in 5 of 7 neurons with α1 expression, while 0 of 12 neurons with α2 also expressed β2 and only one expressed γ2. We address this clustering, as well as the relationship between the developmental trajectories of IPSC kinetics and subunit expression, in DISCUSSION.

Depolarized reversal potential of $GABA_A$ receptors in immature BLA principal neurons. We next examined the effect of age on the $GABA_A$ reversal potential in BLA principal neurons (Fig. 6). Here $GABA_A$ receptor-mediated inhibitory PSPs (IPSPs) were elicited with bipolar stimulation of the dorsolateral BLA in the presence of a cocktail of neurotransmitter receptor antagonists for AMPA/kainate, NMDA, and $GABA_B$ receptors (see MATERIALS AND METHODS). The residual monosynaptic IPSP evoked in the presence of this cocktail was completely abolished by the $GABA_A$ receptor antagonist SR95531 (5 μM, data not shown). The reversal potential of the $GABA_A$ response was estimated with peak IPSP amplitudes from stimulation at three different baseline membrane potentials. This approach corroborated our initial observations, with the $GABA_A$ reversal potential exhibiting a significant hyperpolarizing shift with age (Fig. 6, *A* and *B*; 1-way ANOVA, $F_{3,21} = 19.91$, $P < 0.0001$). For example, the reversal potential was significantly reduced from -54.3 ± 1.0 mV at P7 ($n = 8$) to -66.6 ± 2.3 mV at P14 (Tukey's posttests, $P < 0.001$; $n = 7$). From P14 onward, the mean reversal potential did not change significantly but became less variable across neurons, reaching -69.1 ± 2.0 mV at P21 ($n = 5$) and -69.7 ± 0.9 mV at P28 ($n = 5$). While the whole cell patch-clamp technique is not ideal for measuring $GABA_A$ reversal potentials because of dialysis of the intracellular chloride concentration (which would bias the results for every neuron, regardless of age, toward the Nernst reversal of approximately -33 mV), the observed trend of more hyperpolarizing $GABA_A$ responses with age was robust to the bias. Interestingly, despite the depolarized reversal potential of $GABA_A$ receptors at P7, we were unable to elicit action potentials with these evoked, isolated $GABA_A$ PSPs in P7 neurons, even when depolarized toward action potential threshold ($n = 4$, data not shown).

The reversal potential of the $GABA_A$-mediated IPSP is influenced by the intracellular concentration of chloride ions,

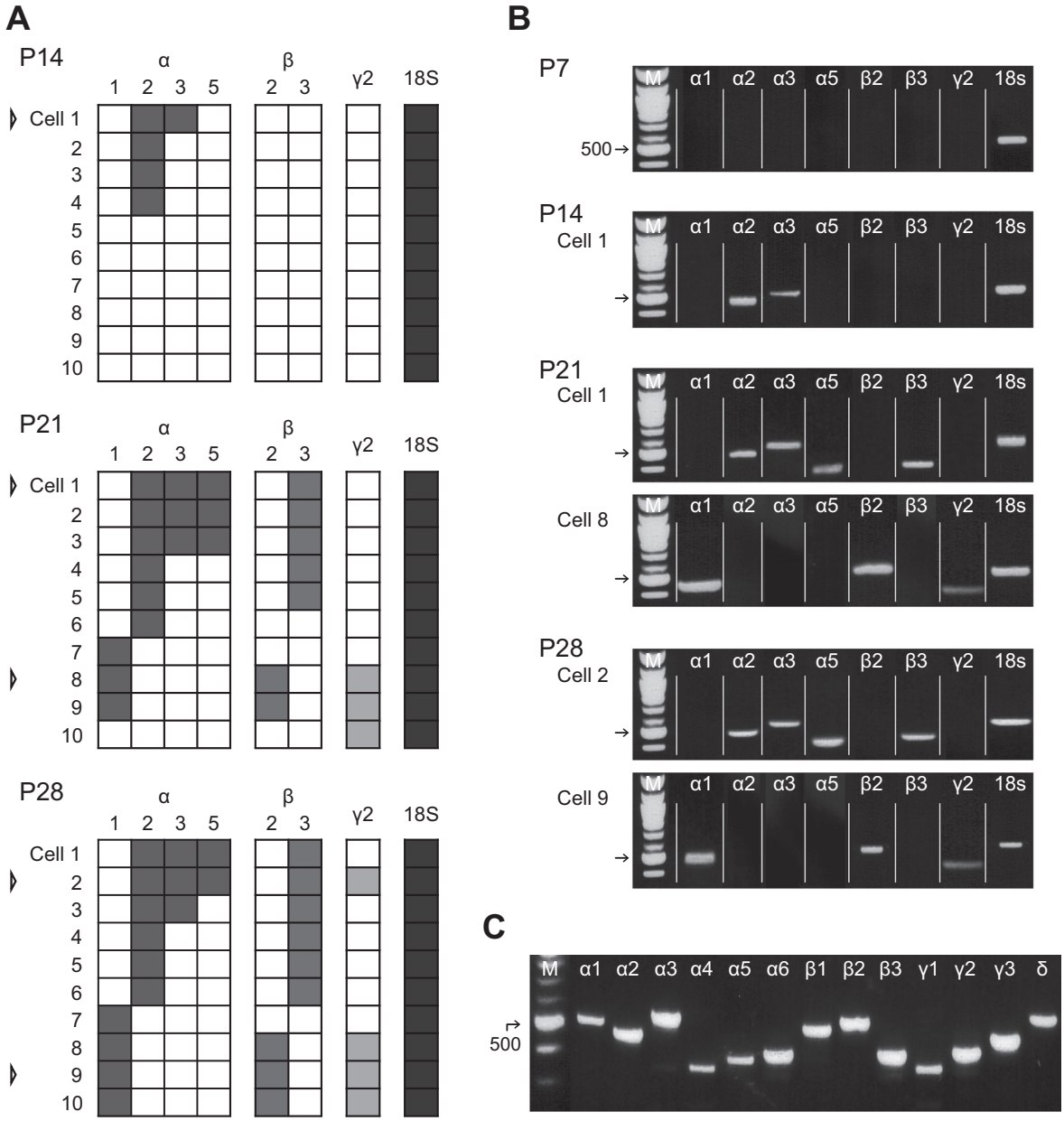

Fig. 5. Development of $GABA_A$ receptor subunit gene expression. *A*: expression of mRNA for 7 $GABA_A$ receptor subunits ($\alpha1$, $\alpha2$, $\alpha3$, $\alpha5$, $\beta2$, $\beta3$, and $\gamma2$) is depicted for 10 BLA principal neurons at P14, P21, and P28. Each row depicts the expression of each gene for a single neuron, with positive signal represented by a filled box. Ten neurons at P7 were also analyzed but are not presented because they lacked detectable expression for all genes but 18S. Only neurons with signal for the housekeeper gene 18S rRNA were included. Gel pictures are presented for representative neurons identified by open arrowheads. *B*: gel pictures depict the expression of particular receptor subunits for 1 or 2 representative neurons at each time point, reassembled from gels organized by gene instead of individual neuron. *C*: gel picture showing detectable mRNA expression for all $GABA_A$ receptor subunits tested in whole BLA from a representative animal at P7 ($n = 4$).

which is tightly regulated by the activity of two selective ion pumps: NKCC1, which promotes excitatory $GABA_A$ receptor-mediated potentials, and KCC2, which facilitates an inhibitory response to $GABA_A$ receptor activation. The expression of these pumps is developmentally regulated, and we were therefore interested in the developmental trajectory of chloride pump expression in BLA principal neurons. Using single-cell RT-PCR, we measured the expression at P7, P14, P21, and P28. Consistent with the depolarized reversal potential we observed in immature neurons, there was a shift in mRNA expression from NKCC1 to KCC2 between P7 and P21 (Fig. 6*D*). Specifically, there was comparable expression of the two transcripts at P7, with 9 and 10 of 15 neurons expressing detectable levels of NKCC1 and KCC2, respectively. At P14, NKCC1 was more prominent, expressed by 17 of 20 neurons compared with only 5 of 20 with KCC2 expression. No NKCC1 transcripts were detected at P21 or P28, but the majority of neurons expressed KCC2 (21 of 23 at P21, 5 of 8 at P28).

Short-term plasticity of $GABA_A$ IPSCs. The influence of GABA on BLA principal neuron activity depends not only on the amplitude, kinetics, and valence of individual synaptic events but also on the patterning and plasticity of these events. Therefore, we next characterized the development of STP of

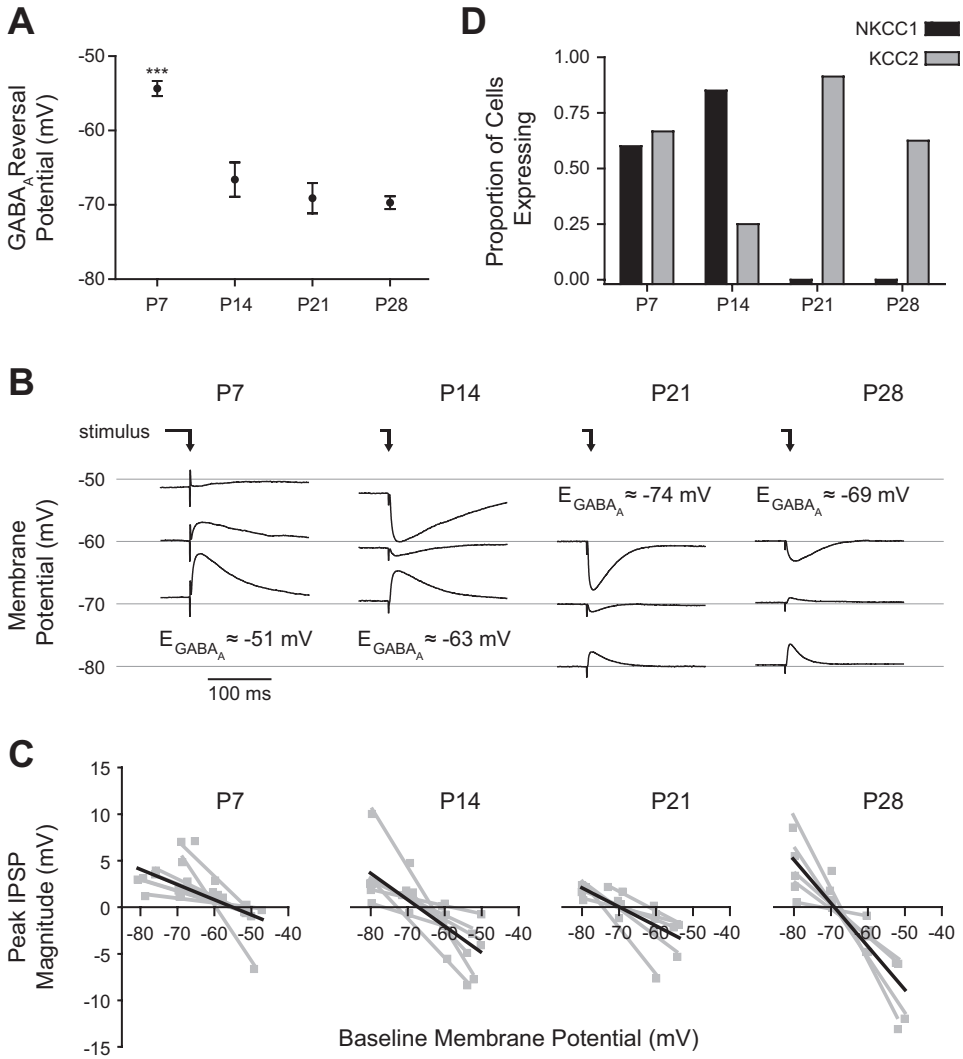

Fig. 6. Maturation of $GABA_A$ reversal potential and chloride pump expression. *A* and *B*: reversal potential of evoked $GABA_A$ postsynaptic potentials (PSPs) is plotted as mean ± SE (*A*) for neurons at P7 ($n = 8$), P14 ($n = 7$), P21 ($n = 5$), and P28 ($n = 5$), and the average response at 3 different baseline membrane potentials is plotted for a representative neuron at each time point (*B*). The reversal potentials (E_{GABA_A})shown in *B* are specific to the individual neurons depicted. Significance was assessed with a 1-way ANOVA ($F_{3,21} = 19.91$), and pairwise comparisons were made with Tukey's posttests (***$P < 0.001$ vs. P14, P21, and P28). The time of stimulation is depicted with an arrow. *C*: the linear fits used to estimate $GABA_A$ reversal potential for each neuron are plotted in gray for neurons at each time point, with the average line for each group plotted in black. *D*: expression of mRNA for the chloride pumps KCC2 and NKCC1, assessed in individual BLA principal neurons with single-cell RT-PCR, is plotted as the proportion of neurons with detectable expression at P7 ($n = 15$), P14 ($n = 20$), P21 ($n = 23$), and P28 ($n = 8$).

$GABA_A$ receptor-mediated synaptic transmission. Isolated $GABA_A$ receptor-mediated IPSCs were evoked, as before, in voltage-clamped neurons at P7, P14, P21, and P28 with electrical stimulation within the BLA and a cocktail of neurotransmitter antagonists. Trains of five pulses were evoked at 10 and 20 Hz, and the amplitudes of the $GABA_A$ IPSCs within each train were measured (Fig. 7). At both 10- and 20-Hz stimulation, IPSCs at P7 exhibited robust short-term depression (Fig. 7, *A* and *B*). The depression was lost gradually with age. Because of this gradation, we included a group of neurons at P35 to determine whether the trend reached an asymptote at P28.

To quantify the developmental changes, we used two metrics based on IPSC amplitudes: the early STP, defined as the ratio of the amplitudes of the second and first IPSCs in the train, and the late STP, defined as the ratio of the fifth and first IPSCs in the train (Table 2). For early STP, there was a significant main effect of age (2-way ANOVA with repeated measures, $F_{4,23} = 8.53$, $P < 0.001$) but no effect of stimulation frequency (Fig. 7*C*). All possible pairwise comparisons were made with Bonferroni posttests. For 10-Hz stimulation, early STP exhibited no significant developmental transitions. However, significant individual transitions were found for 20-Hz stimulation. Specifically, early STP for 20-Hz stimulation increased significantly from P7 to P21 ($P < 0.05$), P28 ($P < 0.001$), and P35 ($P < 0.001$). There were also significant increases from P14 to P28 ($P < 0.05$) and P35 ($P < 0.01$) and from P21 to P35 ($P < 0.01$). For both stimulation frequencies the values at P28 and P35 were highly similar, suggesting that the phenotype is stable beyond P28.

Late STP, the ratio of the fifth IPSC to the first, also exhibited robust synaptic depression in immature neurons that transitioned toward synaptic facilitation with age. A two-way ANOVA with repeated measures revealed significant main effects of age ($F_{4,23} = 3.709$, $P < 0.05$) and stimulation frequency ($F_{1,23} = 14.58$, $P < 0.001$) as well as a significant interaction effect ($F_{4,23} = 3.29$, $P < 0.05$; Fig. 7*D*). Pulse ratios for 20-Hz stimulation were generally smaller than those for 10 Hz. Late STP for 10-Hz stimulation exhibited an increase with age, although none of the individual transitions was statistically significant. For 20-Hz stimulation, late STP increased significantly from P7 to P28 ($P < 0.05$). For both stimulation frequencies, $n = 3$ neurons at P7, 5 at P14, 7 at P21, 6 at P28, and 7 at P35.

Spontaneous GABA activity is rhythmically organized throughout the first postnatal month. Finally, although we observed many differences in the character of GABAergic synaptic transmission with age, it is important to consider these changes in the context of normal GABA function. In slice

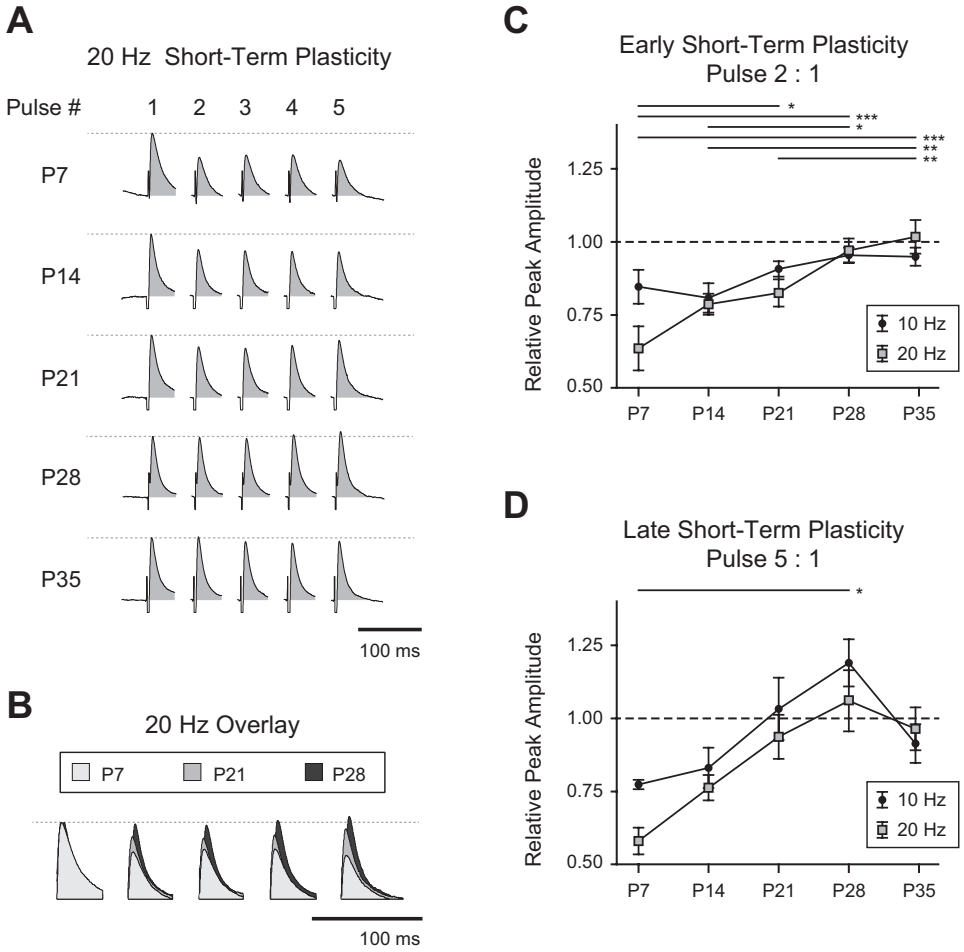

Fig. 7. Development of short-term synaptic plasticity of IPSCs. *A*: short-term plasticity of $GABA_A$ IPSCs in representative neurons at P7, P14, P21, P28, and P35 are illustrated as the average response to stimulation of the dorsolateral BLA with 5 pulses at 20 Hz. Neurotransmitter receptor antagonists were used to isolate the $GABA_A$ component of the response (see MATERIALS AND METHODS). Stimulation responses were aligned to and normalized by the first pulse, and stimulation artifacts were cropped for clarity. The area under the curve was filled to aid visual comparison across time points. *B*: as in *A*, average, normalized IPSCs in response to 20-Hz stimulation are overlaid for comparison, taken from a representative neuron at P7, P21, and P28. *C* and *D*: short-term plasticity was quantified for 10-Hz and 20-Hz stimulation as a ratio of pulse amplitudes. The ratios of the second pulse (early STP, *C*) and fifth pulse (late STP, *D*) to the first pulse are plotted for each time point as means ± SE. Significance was assessed with 2-way ANOVAs with repeated measures, and all pairwise comparisons were made with Bonferroni posttests. Bars above each plot illustrate the significant pairwise comparisons for stimulation at 20 Hz ($*P < 0.05$, $**P < 0.01$, $***P < 0.001$). No pairwise comparisons for 10-Hz stimulation were significant. $n = 3$ (P7), 5 (P14), 7 (P21), 6 (P28), and 7 (P35).

preparations of the adult BLA, groups of principal neurons simultaneously receive rhythmic, compound synaptic events that consist mainly of $GABA_A$ receptor-mediated IPSCs but also include glutamatergic EPSCs. We have observed them not only in BLA slices from adult rats but also in rhesus macaques, where they promote intrinsic membrane potential oscillations and coordinate network activity (Ryan et al. 2012). Considering the important functional role of these synaptic events, we characterized their expression during postnatal development (Fig. 8). We observed rhythmic, compound IPSCs as early as P7 and at every time point studied (Fig. 8, *A* and *B*). As expected, the rhythmic PSCs were depolarizing from rest at P7 and became consistently hyperpolarizing by P21. The waveform changed with age, as rhythmic IPSCs at P7 were smooth while those at P28 were sharp, a cluster of many distinct release events (Fig. 8*A*). Interestingly, the proportion of neurons receiving compound IPSCs was similar at all ages, with rhythmic events spontaneously observed in ~20–40% of neurons (6 of 14 neurons at P7, 6 of 28 at P14, 8 of 25 at P21, and 4 of 16 at P28; Fig. 8*B*). Consistent with the mature BLA (Ryan et al. 2012), as early as P7 rhythmic IPSCs were perfectly synchronized across BLA principal neurons (Fig. 8*C*).

Table 2. *IPSC amplitude ratios for short-term plasticity*

	Early STP		Late STP	
	10 Hz	20 Hz	10 Hz	20 Hz
P7	0.84 ± 0.06	0.64 ± 0.08	0.77 ± 0.02	0.58 ± 0.05
P14	0.81 ± 0.05	0.78 ± 0.04	0.83 ± 0.07	0.76 ± 0.04
P21	0.91 ± 0.03	0.83 ± 0.05	1.03 ± 0.11	0.94 ± 0.08
P28	0.95 ± 0.03	0.97 ± 0.04	1.19 ± 0.08	1.06 ± 0.10
P35	0.95 ± 0.03	1.02 ± 0.06	0.91 ± 0.07	0.96 ± 0.07

Ratios of inhibitory postsynaptic current (IPSC) amplitudes after 10- and 20-Hz stimulation are listed for each time point as means ± SE. Early short-term plasticity (STP) corresponds to the ratio of *pulse 2* to *pulse 1* and late STP to the ratio of *pulse 5* to *pulse 1*. Statistical tests for significance are described in RESULTS. P, postnatal day.

DISCUSSION

In this study, we provided the first evidence that synaptic transmission, in particular GABAergic transmission, undergoes significant change throughout BLA development. Similar to the intrinsic physiology of BLA principal neurons (Ehrlich et al. 2012), we demonstrated that inhibitory synaptic transmission reaches maturity ~3–4 wk after birth. Specifically, $GABA_A$ receptor-mediated PSCs become faster and more hyperpolarizing and lose short-term depression with age until P21–P28, when rats are in late infancy (Quinn 2005). In addition, these physiological changes correspond with maturation of the expression of genes that influence GABAergic function specifically in BLA principal neurons—in the case of PSC kinetics a change in $GABA_A$ receptor subunit expression and in the case of PSC reversal a shift in chloride transporter expression. Considering the critical role of GABAergic transmission in the function of BLA principal neurons and the

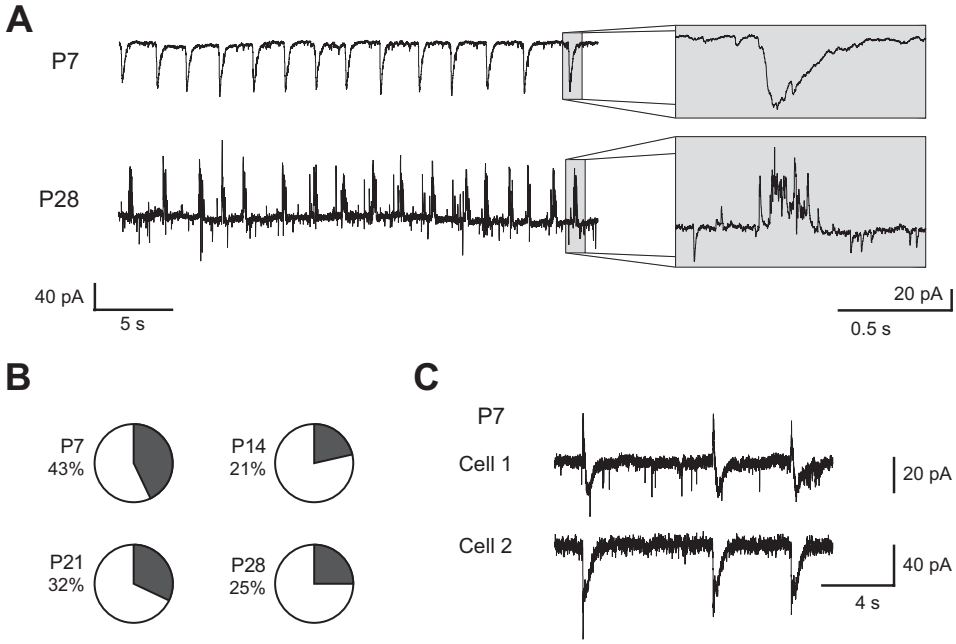

Fig. 8. Maturation of spontaneous, rhythmic IPSCs. *A*: representative BLA principal neurons at P7 and P28 spontaneously exhibit rhythmic, compound IPSCs. Both neurons were recorded in voltage clamp with a holding potential of −60 mV. *Insets* highlight the waveform of individual events. *B*: pie charts depict the proportion of neurons spontaneously receiving rhythmic IPSCs at each time point (n = 14 at P7, 28 at P14, 25 at P21, and 16 at P28). *C*: traces from a pair of simultaneously recorded BLA principal neurons illustrate that rhythmic IPSCs are synchronized across BLA principal neurons as early as P7.

nucleus in general, these changes likely contribute to the maturation of amygdala function throughout postnatal development.

Shift from depolarizing to hyperpolarizing $GABA_A$ transmission. One of the most profound changes we observed in the developing BLA was a transition in the $GABA_A$ reversal potential. The reversal potential in principal neurons became more hyperpolarized with age, shifting from approximately −55 mV at P7 to −70 mV at P21. The magnitude and time course of this change matched those identified in cell-attached recordings of hippocampal pyramidal neurons, which exhibit a similar hyperpolarization of the $GABA_A$ reversal potential of ~15 mV between birth and P17 (Tyzio et al. 2008). The existence of excitatory $GABA_A$ receptor-mediated potentials during brain development has been well documented (Ben-Ari 2002; Owens and Kriegstein 2002). In BLA principal neurons before P14, $GABA_A$ receptor activation caused depolarization, suggesting that these receptors play a different functional role early in development. Depolarizing $GABA_A$ receptors should render the BLA more excitable, which may be important for communication between the BLA and other limbic brain regions like the extended amygdala, hippocampus, and prefrontal cortex, before strong connections have been formed (Bouwmeester et al. 2002a, 2002b). One consequence of depolarizing $GABA_A$ receptors is that positive allosteric modulators like barbiturates and benzodiazepines could paradoxically facilitate activation of BLA principal neurons during infancy, which could have important clinical ramifications, particularly in light of the role of the BLA as an epileptogenic locus and the incidence of infantile seizures (Racine et al. 1972; White and Price 1993).

Depolarizing $GABA_A$ transmission likely serves an important function in normative brain development: $GABA_A$ receptors are thought to fulfill the role AMPA receptors play in the mature brain, providing sufficient postsynaptic depolarization to enable NMDA receptor activation and subsequent synaptic strengthening (Ben-Ari et al. 1997, 2012). This phenomenon likely occurs in the immature BLA when glutamate and GABA are simultaneously released during the rhythmic, compound PSCs we described here. Rhythmic, compound PSCs could serve this purpose in the BLA as early as P7, with 43% of neurons recorded at P7 receiving them. Supporting this notion, synaptic events in the immature hippocampus similar to our rhythmic PSCs, termed "giant depolarizing potentials," have been shown to promote synaptic strengthening (Mohajerani and Cherubini 2006). This function of rhythmic PSCs is distinct from that proposed in the adult BLA, where rhythmic IPSCs promote intrinsic membrane potential oscillations and synchronize action potentials across BLA principal neurons (Ryan et al. 2012). Interestingly, mature oscillatory properties of BLA principal neurons are not present until around P21 (Ehrlich et al. 2012), supporting convergent developmental timing of inhibitory GABA and membrane potential oscillations. In the mature BLA rhythmic IPSCs are driven by a syncytium of burst-firing parvalbumin interneurons (Rainnie et al. 2006), but parvalbumin expression does not emerge in the BLA until around P14 (Berdel and Moryś 2000); rhythmic PSCs at P7 may be driven by burst-firing interneurons that may later express parvalbumin.

A possible caveat to our measurements of reversal potential is that dialysis of the cytosol by our patch solution could alter the electrochemical gradients of ions passed by $GABA_A$ receptors, particularly chloride. However, if dialysis had an effect, it would be to minimize differences across time points, shifting the reversal potential toward the Nernst reversal of chloride, approximately −33 mV for our patch solution and ACSF. The disparity between the observed reversals and the Nernst reversal, as well as the significant effect we found of age on $GABA_A$ reversal, suggests that the chloride concentration near $GABA_A$ receptors is locally regulated. Interestingly, there is a precedent for chloride reversal being robust to dialysis of the neuronal cytosol (Gonzalez-Islas et al. 2009; Jarolimek et al. 1999). Therefore, we are confident in our observations of a hyperpolarization of the $GABA_A$ reversal with age.

Hyperpolarization of the $GABA_A$ reversal potential with age is typically thought to result from a change in the expression of

chloride pumps from NKCC1, which renders $GABA_A$ excitatory by extruding chloride, to KCC2, which renders it inhibitory by accumulating the ion intracellularly (Ben-Ari et al. 2002). Indeed, our single-cell RT-PCR study indicated that at P7 and P14 a high proportion of principal neurons express mRNA for NKCC1, but expression was undetectable by P21. In contrast, mRNA for KCC2 was prominent at P21 and P28. These changes in chloride pump expression are also consistent with those in other brain regions (Ben-Ari et al. 2002). Further experiments will be required to determine whether levels of protein expression follow suit and whether similar changes in chloride pump expression occur in BLA interneurons.

Development of a GABAergic shunt of the network response. Corresponding with the emergence of inhibitory $GABA_A$ potentials was a shortening of the network response to local electrical stimulation. Specifically, in immature neurons low-frequency stimulation evoked slow, depolarizing $GABA_A$ responses and even slower, inhibitory $GABA_B$ responses resulting in a compound potential that could last between 1 and 2 s. By P21 the mature phenotype was present, in which stimulation evoked a fast, inhibitory $GABA_A$ response followed by a curtailed $GABA_B$ response, returning to baseline within 1 s (Rainnie et al. 1991; Washburn and Moises 1992). Although we have previously reported that immature neurons have larger input resistances and membrane time constants (Ehrlich et al. 2012), this did not fully account for the slower synaptic potentials. Our voltage-clamp recordings also revealed a prolongation of stimulation-evoked $GABA_A$ currents in immature neurons.

The long duration of the network response in immature neurons likely results from the depolarized reversal potential of $GABA_A$ receptors. In adult BLA principal neurons, feedforward activation of inhibitory $GABA_A$ receptors provides a fast shunt, limiting the extent of BLA activation (Rainnie et al. 1991). As we have shown here, in immature BLA principal neurons $GABA_A$ is depolarizing, which should enable or even promote feedforward excitation within the BLA. Without feedforward $GABA_A$ receptor-mediated inhibition, in the immature BLA a different brake is afforded: potent activation of $GABA_B$ receptors. However, $GABA_B$ acts on a slower timescale than $GABA_A$, which would explain the long-duration network responses observed here. The strong $GABA_B$ receptor activation we found at P7 could mitigate the risk of hyperexcitability and excitotoxicity due to GABA release by opposing the depolarizing action of $GABA_A$ at this age.

$GABA_B$ receptors are thought to be localized extrasynaptically, and in adulthood they are activated when a train of stimuli releases sufficient GABA to spill over into the extrasynaptic compartment (Beenhakker and Huguenard 2010; Fritschy et al. 1999; Kim et al. 1997; Kulik et al. 2002; Scanziani 2000). The strong $GABA_B$ response to a single stimulation in the immature BLA suggests there is an age-dependent difference in the accessibility of GABA to $GABA_B$ receptors after stimulation. This developmental change must be interpreted in the context of the concurrent increase in input resistance, but the amplitude of $GABA_B$ relative to $GABA_A$ PSPs decreases considerably with age. This difference could be afforded by age-dependent changes in the architecture of GABAergic synapses. To support this notion, $GABA_B$ receptors in cerebellar neurons move from dendritic shafts at P7 to spines at P21 (Lujan and Shigemoto 2006). Moreover, activation of metabotropic receptors with a single stimulation may be a general phenomenon early in development; we observed a muscarinic current that was abolished by atropine (5 μM) and evoked by single stimulation in some neurons at P7 but not at any later time points (unpublished observation).

Faster IPSCs with age. The function of GABA in the BLA also depends on the kinetics of $GABA_A$ receptor-mediated IPSCs, and we found significant developmental changes to their kinetics. Specifically, there was a nearly twofold reduction in spontaneous IPSC rise time from P7 to P21, when the mature, fast waveform was expressed. Decay time constant and IPSC half-width exhibited a similar trajectory. As with the decay time constant of spontaneous IPSCs, there was an abrupt decrease from P14 to P21 in the kinetics of the response to exogenous muscimol. Interestingly, while the peak conductance of the response to muscimol significantly increased with age, we found no age-dependent change in the peak conductance underlying spontaneous IPSCs. This effect may be due to the proximity of receptor activation to the soma, since the picospritzer pipette was placed close to the soma while IPSCs presumably originate throughout the dendritic arbor. This notion is supported by the fact that dendrites of BLA principal neurons expand greatly throughout the first postnatal month, with the total dendritic length increasing more than threefold as dendrites come to extend more than twice as far from the soma (Ryan et al., unpublished observations). Furthermore, this difference may be due to a developmental change in the ratio of synaptic to extrasynaptic $GABA_A$ receptors.

When considered in the context of a nearly threefold reduction in membrane time constant from P7 to P28, $GABA_A$ PSPs are likely much faster in the adult BLA (Ehrlich et al. 2012). The presence of slow IPSCs early in development has been well documented throughout the brain (Draguhn and Heinemann 1996; Dunning et al. 1999; Hollrigel and Soltesz 1997; Pouzat and Hestrin 1997). Comparable developmental changes were also found in the kinetics of miniature IPSCs in marmoset amygdala principal neurons, albeit on a different time course (Yamada et al. 2012). The kinetics of individual IPSCs should influence their effect on spike timing (Pouille and Scanziani 2001) and are known to regulate the ability of GABAergic afferents to entrain postsynaptic oscillations (Tamas et al. 2004). Furthermore, faster IPSCs should more precisely control the timing of spikes and membrane potential oscillations due to postinhibitory rebound (Ryan et al. 2012), promoting the viability of temporal coding mechanisms in the adult BLA.

The maturation of IPSC kinetics corresponds with changes to the expression of $GABA_A$ receptor subunits in BLA principal neurons. We observed an increase with age in the proportion of neurons expressing seven different $GABA_A$ subunits. The subunit mRNA we found in BLA principal neurons at P21 and P28 closely matches protein expression in the adult BLA, aside from the α4-, β1-, and δ-subunits (Sieghart and Sperk 2002). Expression of α4, β1, and δ is likely found in other cell types. Expression of the α1-subunit, among others, emerged at P21, confirming results found with mRNA from whole BLA (Zhang et al. 1992). This change is well documented throughout the brain and is known to contribute to the faster kinetics observed with age (Bosman et al. 2002; Davis et al. 2000; Dunning et al. 1999; Eyre et al. 2012; Hornung and Fritschy 1996; Mohler et al. 2004; Okada et al. 2000; Vicini et al. 2001). Developmental changes in subunit expression are also known

to regulate channel localization and drug sensitivity (Hevers and Luddens 2002; Nusser et al. 1996). Activation of receptors containing the $GABA_A$ receptor α1-subunit directly influence critical period onset (Fagiolini et al. 2004; Huntsman et al. 1994), suggesting that the emergence of α1 expression may trigger other aspects of emotional circuit development. Despite the apparent contribution of postsynaptic changes, identified with exogenous muscimol application, to the development of IPSC kinetics, the observed maturation of IPSC kinetics may be due, in part, to changes in the activity of different subtypes of interneurons. This notion is supported by the fact that interneurons exhibit specificity in the subunit composition of $GABA_A$ receptors to which they are apposed. For instance, in the hippocampus synapses formed by parvalbumin-expressing interneurons on pyramidal cell somas preferentially express the $GABA_A$ receptor α1-subunit (Klausberger et al. 2002). In the BLA, parvalbumin-expressing interneurons do not emerge until P17 and reach maturity at P30 (Berdel and Moryś 2000), which corresponds with the emergence of α1 expression between P14 and P21 observed here.

We also observed clustering of subunit expression at P21 and P28, with α1-, β2-, and γ2-subunits primarily expressed in distinct neurons from α2, α3, α5, and β3. While this result was unexpected and curious considering the homogeneous population of $GABA_A$ PSCs we observed, there is some precedent for separation of α1 protein from other α-subunits (Hutcheon et al. 2004). There is an important caveat for interpreting this clustering, namely, the high rate of false negatives. Similarly, while neurons at P7 provided enough RNA to detect 18S and chloride pump expression, the lack of $GABA_A$ subunit mRNA detected is not evidence for an absolute lack of $GABA_A$ receptors. The presence of $GABA_A$ receptor-mediated PSCs and receptor subunit mRNA in whole tissue at P7 clearly refutes this, meaning that the developmental changes we see in subunit transcript expression are not concrete but indicate trends in expression levels. As with all single-cell RT-PCR results, it will be important to extend these findings by quantifying mRNA and protein expression in the developing BLA.

Short-term synaptic depression of $GABA_A$ IPSCs in immature BLA. We also found distinct changes to GABAergic synaptic plasticity during development. At P7, $GABA_A$ inputs to BLA principal neurons exhibited robust early and late synaptic depression. Gradually with age the synaptic depression waned and shifted toward short-term facilitation. By P28, the amplitude of the response was maintained at the second pulse (early STP) and facilitated at the fifth (late STP). Comparable changes on a similar developmental trajectory have been observed for GABAergic and glutamatergic synapses in other brain regions (Pouzat and Hestrin 1997; Reyes and Sakmann 1999). For late STP, we observed facilitation at P28 that disappeared by P35; while this trend was not significant, it raises the interesting possibility of a temporary window with short-term facilitation around P28. There was also a significant effect of stimulation frequency on late STP. Short-term depression is classically sensitive to stimulation frequency, likely because of the kinetics of depletion and restoration of releasable neurotransmitter pools (Elfant et al. 2008; Zucker and Regehr 2002). Interestingly, for late STP there was also a significant interaction effect; the influence of stimulation frequency on STP decreased with age and may therefore be specific to short-term depression.

The developmental change in STP may be explained by several mechanisms, although the simplest involves a change in release probability—from high-release-probability, high-output GABAergic terminals in immature neurons to low release probability, low output in the mature BLA (for review see Zucker and Regehr 2002). High GABAergic output would be parsimonious with the robust activation of $GABA_B$ receptors we observed in immature BLA principal neurons. In light of this hypothesis, future studies should address the contribution of parvalbumin expression to STP in the BLA. This calcium-binding protein directly influences STP and presynaptic calcium dynamics (Collin et al. 2005; Eggermann and Jonas 2012; Vreugdenhil et al. 2003), and its expression in the BLA changes during the first postnatal month (Berdel and Moryś 2000). We can rule out a contribution of presynaptic $GABA_B$ receptors to the observed short-term depression in younger animals, because CGP52432 was included in the bath during these experiments; however, presynaptic $GABA_A$ receptors can play a similar role (MacDermott et al. 1999). $GABA_A$ receptor desensitization is also known to contribute to short-term depression (Overstreet et al. 2000), although there is no precedent for a developmental change in this phenomenon. Finally, short-term depression of immature GABAergic IPSCs may involve ionic plasticity, a depolarization of the chloride reversal following strong $GABA_A$ activation (for review see Raimondo et al. 2012). To better understand the maturation of STP we observed, future studies should differentiate the various interneuron subtypes found in the BLA, which play different roles in the network but were grouped in the population response used here.

STP affords synapses with a variety of temporal filtering mechanisms, suggesting that the BLA processes information and communicates using different mechanisms with age (Buonomano 2000; Fortune and Rose 2001; Pfister et al. 2010). The role of synaptic filters in tuning the network to specific frequencies is particularly important because BLA oscillations have been implicated in the expression and consolidation of fear memories (Lesting et al. 2011; Madsen and Rainnie 2009; Popa et al. 2010; Sangha et al. 2009) and BLA inhibition is thought to promote these oscillations (Ryan et al. 2012). Short-term depression of inhibition, as we observed in the juvenile BLA, promotes high-pass filtering of excitatory input and increases the information transmitted by bursts (Abbott and Regehr 2004; George et al. 2011). Therefore, short-term depression may provide salience for high-frequency and bursting activity in the immature BLA, possibly providing compensation for the reduced sensitivity to high-frequency input of immature BLA principal neurons (Ehrlich et al. 2012).

We have shown that synaptic inhibition in the developing BLA is not static but undergoes a number of profound changes that will directly influence BLA physiology and its contribution to emotional processing. The function of GABA receptors and, therefore, of the entire BLA are in flux during the first postnatal month, which likely contributes to the emotional changes observed during this window. To improve our understanding of the etiology of psychiatric disorders, it will be important to characterize how the normative development of the amygdala is influenced by genetic predispositions and risk factors for psychiatric disease (Monk 2008; Pine 2002). Furthermore, future studies should determine whether development of synaptic transmission in the amygdala contributes to

the expression of critical periods that render the brain vulnerable to the pathogenesis of emotional disorders like anxiety, depression, and autism spectrum disorders.

ACKNOWLEDGMENTS

The authors thank Prof. Peter Wenner for his constructive comments on the manuscript.

GRANTS

This work was funded by the following grants from the National Institutes of Health: Grant MH-069852 to D. G. Rainnie, Base Grant RR-00165 to the Yerkes National Primate Research Center, and Grant MH-090729 to D. E. Ehrlich.

DISCLOSURES

No conflicts of interest, financial or otherwise, are declared by the author(s).

AUTHOR CONTRIBUTIONS

Author contributions: D.E.E., S.J.R., and D.G.R. conception and design of research; D.E.E., S.J.R., R.H., and J.-D.G. performed experiments; D.E.E., S.J.R., and R.H. analyzed data; D.E.E. and D.G.R. interpreted results of experiments; D.E.E. prepared figures; D.E.E. drafted manuscript; D.E.E., S.J.R., R.H., and D.G.R. edited and revised manuscript; D.E.E., S.J.R., R.H., J.-D.G., and D.G.R. approved final version of manuscript.

REFERENCES

Abbott LF, Regehr WG. Synaptic computation. *Nature* 431: 796–803, 2004.

Adolphs R, Baron-Cohen S, Tranel D. Impaired recognition of social emotions following amygdala damage. *J Cogn Neurosci* 14: 1264–1274, 2002.

Baron-Cohen S, Ring HA, Bullmore ET, Wheelwright S, Ashwin C, Williams SC. The amygdala theory of autism. *J Neurosci* 24: 355–364, 2000.

Beenhakker MP, Huguenard JR. Astrocytes as gatekeepers of $GABA_B$ receptor function. *J Neurosci* 30: 15262–15276, 2010.

Ben-Ari Y. Excitatory actions of GABA during development: the nature of the nurture. *Nat Rev Neurosci* 3: 728–739, 2002.

Ben-Ari Y, Khalilov I, Kahle KT, Cherubini E. The GABA excitatory/inhibitory shift in brain maturation and neurological disorders. *Neuroscientist* 18: 467–486, 2012.

Ben-Ari Y, Khazipov R, Leinekugel X, Caillard O, Gaiarsa JL. $GABA_A$, NMDA and AMPA receptors: a developmentally regulated "menage a trois." *Trends Neurosci* 20: 523–529, 1997.

Berdel B, Moryś J. Expression of calbindin-D28k and parvalbumin during development of rat's basolateral amygdaloid complex. *Int J Dev Neurosci* 18: 501–513, 2000.

Bosman LW, Rosahl TW, Brussaard AB. Neonatal development of the rat visual cortex: synaptic function of $GABA_A$ receptor alpha subunits. *J Physiol* 545: 169–181, 2002.

Bouwmeester H, Smits K, Van Ree JM. Neonatal development of projections to the basolateral amygdala from prefrontal and thalamic structures in rat. *J Comp Neurol* 450: 241–255, 2002a.

Bouwmeester H, Wolterink G, van Ree JM. Neonatal development of projections from the basolateral amygdala to prefrontal, striatal, and thalamic structures in the rat. *J Comp Neurol* 442: 239–249, 2002b.

Brummelte S, Witte V, Teuchert-Noodt G. Postnatal development of GABA and calbindin cells and fibers in the prefrontal cortex and basolateral amygdala of gerbils (*Meriones unguiculatus*). *Int J Dev Neurosci* 25: 191–200, 2007.

Buonomano DV. Decoding temporal information: a model based on short-term synaptic plasticity. *J Neurosci* 20: 1129–1141, 2000.

Campbell BA, Ampuero MX. Dissociation of autonomic and behavioral components of conditioned fear during development in the rat. *Behav Neurosci* 99: 1089–1102, 1985.

Chattopadhyaya B, Cristo GD. GABAergic circuit dysfunctions in neurodevelopmental disorders. *Front Psychiatry* 3: 51, 2012.

Collin T, Chat M, Lucas MG, Moreno H, Racay P, Schwaller B, Marty A, Llano I. Developmental changes in parvalbumin regulate presynaptic Ca^{2+} signaling. *J Neurosci* 25: 96–107, 2005.

Davila JC, Olmos L, Legaz I, Medina L, Guirado S, Real MA. Dynamic patterns of colocalization of calbindin, parvalbumin and GABA in subpopulations of mouse basolateral amygdalar cells during development. *J Chem Neuroanat* 35: 67–76, 2008.

Davis AM, Penschuck S, Fritschy JM, McCarthy MM. Developmental switch in the expression of $GABA_A$ receptor subunits $alpha_1$ and $alpha_2$ in the hypothalamus and limbic system of the rat. *Brain Res Dev Brain Res* 119: 127–138, 2000.

Davis M, Rainnie D, Cassell M. Neurotransmission in the rat amygdala related to fear and anxiety. *Trends Neurosci* 17: 208–214, 1994.

Davis M, Walker DL, Myers KM. Role of the amygdala in fear extinction measured with potentiated startle. *Ann NY Acad Sci* 985: 218–232, 2003.

Draguhn A, Heinemann U. Different mechanisms regulate IPSC kinetics in early postnatal and juvenile hippocampal granule cells. *J Neurophysiol* 76: 3983–3993, 1996.

Dunning DD, Hoover CL, Soltesz I, Smith MA, O'Dowd DK. $GABA_A$ receptor-mediated miniature postsynaptic currents and alpha-subunit expression in developing cortical neurons. *J Neurophysiol* 82: 3286–3297, 1999.

Eggermann E, Jonas P. How the "slow" Ca^{2+} buffer parvalbumin affects transmitter release in nanodomain-coupling regimes. *Nat Neurosci* 15: 20–22, 2012.

Ehrlich DE, Ryan SJ, Rainnie DG. Postnatal development of electrophysiological properties of principal neurons in the rat basolateral amygdala. *J Physiol* 590: 4819–4838, 2012.

Ehrlich I, Humeau Y, Grenier F, Ciocchi S, Herry C, Luthi A. Amygdala inhibitory circuits and the control of fear memory. *Neuron* 62: 757–771, 2009.

Elfant D, Pal BZ, Emptage N, Capogna M. Specific inhibitory synapses shift the balance from feedforward to feedback inhibition of hippocampal CA1 pyramidal cells. *Eur J Neurosci* 27: 104–113, 2008.

Eyre MD, Renzi M, Farrant M, Nusser Z. Setting the time course of inhibitory synaptic currents by mixing multiple $GABA_A$ receptor alpha subunit isoforms. *J Neurosci* 32: 5853–5867, 2012.

Fagiolini M, Fritschy JM, Low K, Mohler H, Rudolph U, Hensch TK. Specific $GABA_A$ circuits for visual cortical plasticity. *Science* 303: 1681–1683, 2004.

Fortune ES, Rose GJ. Short-term synaptic plasticity as a temporal filter. *Trends Neurosci* 24: 381–385, 2001.

Fritschy JM, Meskenaite V, Weinmann O, Honer M, Benke D, Mohler H. $GABA_B$-receptor splice variants GB1a and GB1b in rat brain: developmental regulation, cellular distribution and extrasynaptic localization. *Eur J Neurosci* 11: 761–768, 1999.

George AA, Lyons-Warren AM, Ma X, Carlson BA. A diversity of synaptic filters are created by temporal summation of excitation and inhibition. *J Neurosci* 31: 14721–14734, 2011.

Gonzalez-Islas C, Chub N, Wenner P. NKCC1 and AE3 appear to accumulate chloride in embryonic motoneurons. *J Neurophysiol* 101: 507–518, 2009.

Hazra R, Guo JD, Ryan SJ, Jasnow AM, Dabrowska J, Rainnie DG. A transcriptomic analysis of type I-III neurons in the bed nucleus of the stria terminalis. *Mol Cell Neurosci* 46: 699–709, 2011.

Hensch TK. Critical period plasticity in local cortical circuits. *Nat Rev Neurosci* 6: 877–888, 2005.

Hevers W, Luddens H. Pharmacological heterogeneity of gamma-aminobutyric acid receptors during development suggests distinct classes of rat cerebellar granule cells in situ. *Neuropharmacology* 42: 34–47, 2002.

Hollrigel GS, Soltesz I. Slow kinetics of miniature IPSCs during early postnatal development in granule cells of the dentate gyrus. *J Neurosci* 17: 5119–5128, 1997.

Hornung JP, Fritschy JM. Developmental profile of $GABA_A$-receptors in the marmoset monkey: expression of distinct subtypes in pre- and postnatal brain. *J Comp Neurol* 367: 413–430, 1996.

Hunt PS, Richardson R, Campbell BA. Delayed development of fear-potentiated startle in rats. *Behav Neurosci* 108: 69–80, 1994.

Huntsman MM, Isackson PJ, Jones EG. Lamina-specific expression and activity-dependent regulation of seven $GABA_A$ receptor subunit mRNAs in monkey visual cortex. *J Neurosci* 14: 2236–2259, 1994.

Hutcheon B, Fritschy JM, Poulter MO. Organization of GABA receptor alpha-subunit clustering in the developing rat neocortex and hippocampus. *Eur J Neurosci* 19: 2475–2487, 2004.

Jarolimek W, Lewen A, Misgeld U. A furosemide-sensitive K^+-Cl^- cotransporter counteracts intracellular Cl^- accumulation and depletion in cultured rat midbrain neurons. *J Neurosci* 19: 4695–4704, 1999.

Kessler RC, Berglund P, Demler O, Jin R, Merikangas KR, Walters EE. Lifetime prevalence and age-of-onset distributions of DSM-IV disorders in the National Comorbidity Survey Replication. *Arch Gen Psychiatry* 62: 593–602, 2005.

Kilb W. Development of the GABAergic system from birth to adolescence. *Neuroscientist* 18: 613–630, 2012.

Kim JH, McNally GP, Richardson R. Recovery of fear memories in rats: role of gamma-amino butyric acid (GABA) in infantile amnesia. *Behav Neurosci* 120: 40–48, 2006.

Kim JH, Richardson R. The effect of temporary amygdala inactivation on extinction and reextinction of fear in the developing rat: unlearning as a potential mechanism for extinction early in development. *J Neurosci* 28: 1282–1290, 2008.

Kim U, Sanchez-Vives MV, McCormick DA. Functional dynamics of GABAergic inhibition in the thalamus. *Science* 278: 130–134, 1997.

Kim-Cohen J, Caspi A, Moffitt TE, Harrington H, Milne BJ, Poulton R. Prior juvenile diagnoses in adults with mental disorder: developmental follow-back of a prospective-longitudinal cohort. *Arch Gen Psychiatry* 60: 709–717, 2003.

King EC, Pattwell SS, Glatt CE, Lee FS. Sensitive periods in fear learning and memory. *Stress* (May 28, 2013). doi:abs/10.3109/10253890.2013.796355.

Klausberger T, Roberts JD, Somogyi P. Cell type- and input-specific differences in the number and subtypes of synaptic $GABA_A$ receptors in the hippocampus. *J Neurosci* 22: 2513–2521, 2002.

Kulik A, Nakadate K, Nyiri G, Notomi T, Malitschek B, Bettler B, Shigemoto R. Distinct localization of $GABA_B$ receptors relative to synaptic sites in the rat cerebellum and ventrobasal thalamus. *Eur J Neurosci* 15: 291–307, 2002.

LeDoux J. The amygdala. *Curr Biol* 17: R868–R874, 2007.

Lesting J, Narayanan RT, Kluge C, Sangha S, Seidenbecher T, Pape HC. Patterns of coupled theta activity in amygdala-hippocampal-prefrontal cortical circuits during fear extinction. *PloS One* 6: e21714, 2011.

Lujan R, Shigemoto R. Localization of metabotropic GABA receptor subunits GABAB1 and GABAB2 relative to synaptic sites in the rat developing cerebellum. *Eur J Neurosci* 23: 1479–1490, 2006.

MacDermott AB, Role LW, Siegelbaum SA. Presynaptic ionotropic receptors and the control of transmitter release. *Annu Rev Neurosci* 22: 443–485, 1999.

Madsen TE, Rainnie DG. Local field potentials in the rat basolateral amygdala and medial prefrontal cortex show coherent oscillations in multiple frequency bands during fear (Abstract). *Neuroscience Meeting Planner* 2009: 132.4/B88, 2009.

Martina M, Royer S, Pare D. Cell-type-specific GABA responses and chloride homeostasis in the cortex and amygdala. *J Neurophysiol* 86: 2887–2895, 2001.

McDonald AJ. Cortical pathways to the mammalian amygdala. *Prog Neurobiol* 55: 257–332, 1998.

McDonald AJ. Immunohistochemical identification of gamma-aminobutyric acid-containing neurons in the rat basolateral amygdala. *Neurosci Lett* 53: 203–207, 1985.

McDonald AJ. Localization of AMPA glutamate receptor subunits in subpopulations of non-pyramidal neurons in the rat basolateral amygdala. *Neurosci Lett* 208: 175–178, 1996.

McEwen BS. Early life influences on life-long patterns of behavior and health. *Ment Retard Dev Disabil Res Rev* 9: 149–154, 2003.

Mohajerani MH, Cherubini E. Role of giant depolarizing potentials in shaping synaptic currents in the developing hippocampus. *Crit Rev Neurobiol* 18: 13–23, 2006.

Mohler H, Fritschy JM, Crestani F, Hensch T, Rudolph U. Specific $GABA_A$ circuits in brain development and therapy. *Biochem Pharmacol* 68: 1685–1690, 2004.

Monk CS. The development of emotion-related neural circuitry in health and psychopathology. *Dev Psychopathol* 20: 1231–1250, 2008.

Moye TB, Rudy JW. Ontogenesis of trace conditioning in young rats: dissociation of associative and memory processes. *Dev Psychobiol* 20: 405–414, 1987.

Neuhaus E, Beauchaine TP, Bernier R. Neurobiological correlates of social functioning in autism. *Clin Psychol Rev* 30: 733–748, 2010.

Nusser Z, Sieghart W, Benke D, Fritschy JM, Somogyi P. Differential synaptic localization of two major gamma-aminobutyric acid type A receptor alpha subunits on hippocampal pyramidal cells. *Proc Natl Acad Sci USA* 93: 11939–11944, 1996.

Okada M, Onodera K, Van Renterghem C, Sieghart W, Takahashi T. Functional correlation of $GABA_A$ receptor alpha subunits expression with the properties of IPSCs in the developing thalamus. *J Neurosci* 20: 2202–2208, 2000.

Overstreet LS, Jones MV, Westbrook GL. Slow desensitization regulates the availability of synaptic $GABA_A$ receptors. *J Neurosci* 20: 7914–7921, 2000.

Owens DF, Kriegstein AR. Is there more to GABA than synaptic inhibition? *Nat Rev Neurosci* 3: 715–727, 2002.

Pape HC, Pare D. Plastic synaptic networks of the amygdala for the acquisition, expression, and extinction of conditioned fear. *Physiol Rev* 90: 419–463, 2010.

Pfister JP, Dayan P, Lengyel M. Synapses with short-term plasticity are optimal estimators of presynaptic membrane potentials. *Nat Neurosci* 13: 1271–1275, 2010.

Pine DS. Brain development and the onset of mood disorders. *Semin Clin Neuropsychiatry* 7: 223–233, 2002.

Pine DS, Cohen P, Gurley D, Brook J, Ma Y. The risk for early-adulthood anxiety and depressive disorders in adolescents with anxiety and depressive disorders. *Arch Gen Psychiatry* 55: 56–64, 1998.

Popa D, Duvarci S, Popescu AT, Lena C, Pare D. Coherent amygdalocortical theta promotes fear memory consolidation during paradoxical sleep. *Proc Natl Acad Sci USA* 107: 6516–6519, 2010.

Pouille F, Scanziani M. Enforcement of temporal fidelity in pyramidal cells by somatic feed-forward inhibition. *Science* 293: 1159–1163, 2001.

Pouzat C, Hestrin S. Developmental regulation of basket/stellate cell–>Purkinje cell synapses in the cerebellum. *J Neurosci* 17: 9104–9112, 1997.

Quinn R. Comparing rat's to human's age: how old is my rat in people years? *Nutrition* 21: 775–777, 2005.

Quirk GJ, Gehlert DR. Inhibition of the amygdala: key to pathological states? *Ann NY Acad Sci* 985: 263–272, 2003.

Racine RJ, Gartner JG, Burnham WM. Epileptiform activity and neural plasticity in limbic structures. *Brain Res* 47: 262–268, 1972.

Raimondo JV, Markram H, Akerman CJ. Short-term ionic plasticity at GABAergic synapses. *Front Synaptic Neurosci* 4: 5, 2012.

Rainnie DG. Serotonergic modulation of neurotransmission in the rat basolateral amygdala. *J Neurophysiol* 82: 69–85, 1999.

Rainnie DG, Asprodini EK, Shinnick-Gallagher P. Inhibitory transmission in the basolateral amygdala. *J Neurophysiol* 66: 999–1009, 1991.

Rainnie DG, Asprodini EK, Shinnick-Gallagher P. Intracellular recordings from morphologically identified neurons of the basolateral amygdala. *J Neurophysiol* 69: 1350–1362, 1993.

Rainnie DG, Bergeron R, Sajdyk TJ, Patil M, Gehlert DR, Shekhar A. Corticotrophin releasing factor-induced synaptic plasticity in the amygdala translates stress into emotional disorders. *J Neurosci* 24: 3471–3479, 2004.

Rainnie DG, Mania I, Mascagni F, McDonald AJ. Physiological and morphological characterization of parvalbumin-containing interneurons of the rat basolateral amygdala. *J Comp Neurol* 498: 142–161, 2006.

Reyes A, Sakmann B. Developmental switch in the short-term modification of unitary EPSPs evoked in layer 2/3 and layer 5 pyramidal neurons of rat neocortex. *J Neurosci* 19: 3827–3835, 1999.

Ryan SJ, Ehrlich DE, Jasnow AM, Daftary S, Madsen TE, Rainnie DG. Spike-timing precision and neuronal synchrony are enhanced by an interaction between synaptic inhibition and membrane oscillations in the amygdala. *PloS One* 7: e35320, 2012.

Sanders SK, Shekhar A. Regulation of anxiety by $GABA_A$ receptors in the rat amygdala. *Pharmacol Biochem Behav* 52: 701–706, 1995.

Sangha S, Narayanan RT, Bergado-Acosta JR, Stork O, Seidenbecher T, Pape HC. Deficiency of the 65 kDa isoform of glutamic acid decarboxylase impairs extinction of cued but not contextual fear memory. *J Neurosci* 29: 15713–15720, 2009.

Scanziani M. GABA spillover activates postsynaptic $GABA_B$ receptors to control rhythmic hippocampal activity. *Neuron* 25: 673–681, 2000.

Schumann CM, Barnes CC, Lord C, Courchesne E. Amygdala enlargement in toddlers with autism related to severity of social and communication impairments. *Biol Psychiatry* 66: 942–949, 2009.

Shekhar A, Sajdyk TJ, Gehlert DR, Rainnie DG. The amygdala, panic disorder, and cardiovascular responses. *Ann NY Acad Sci* 985: 308–325, 2003.

Shekhar A, Truitt W, Rainnie D, Sajdyk T. Role of stress, corticotrophin releasing factor (CRF) and amygdala plasticity in chronic anxiety. *Stress* 8: 209–219, 2005.

Sieghart W, Sperk G. Subunit composition, distribution and function of $GABA_A$ receptor subtypes. *Curr Top Med Chem* 2: 795–816, 2002.

Steinberg L. Cognitive and affective development in adolescence. *Trends Cogn Sci* 9: 69–74, 2005.

Sullivan RM, Landers M, Yeaman B, Wilson DA. Good memories of bad events in infancy. *Nature* 407: 38–39, 2000.

Sweeten TL, Posey DJ, Shekhar A, McDougle CJ. The amygdala and related structures in the pathophysiology of autism. *Pharmacol Biochem Behav* 71: 449–455, 2002.

Tamas G, Szabadics J, Lorincz A, Somogyi P. Input and frequency-specific entrainment of postsynaptic firing by IPSPs of perisomatic or dendritic origin. *Eur J Neurosci* 20: 2681–2690, 2004.

Tang HH, McNally GP, Richardson R. The effects of FG7142 on two types of forgetting in 18-day-old rats. *Behav Neurosci* 121: 1421–1425, 2007.

Thompson JV, Sullivan RM, Wilson DA. Developmental emergence of fear learning corresponds with changes in amygdala synaptic plasticity. *Brain Res* 1200: 58–65, 2008.

Truitt WA, Sajdyk TJ, Dietrich AD, Oberlin B, McDougle CJ, Shekhar A. From anxiety to autism: spectrum of abnormal social behaviors modeled by progressive disruption of inhibitory neuronal function in the basolateral amygdala in Wistar rats. *Psychopharmacology (Berl)* 191: 107–118, 2007.

Tyzio R, Minlebaev M, Rheims S, Ivanov A, Jorquera I, Holmes GL, Zilberter Y, Ben-Ari Y, Khazipov R. Postnatal changes in somatic gamma-aminobutyric acid signalling in the rat hippocampus. *Eur J Neurosci* 27: 2515–2528, 2008.

Vicini S, Ferguson C, Prybylowski K, Kralic J, Morrow AL, Homanics GE. $GABA_A$ receptor alpha1 subunit deletion prevents developmental changes of inhibitory synaptic currents in cerebellar neurons. *J Neurosci* 21: 3009–3016, 2001.

Vreugdenhil M, Jefferys JG, Celio MR, Schwaller B. Parvalbumin-deficiency facilitates repetitive IPSCs and gamma oscillations in the hippocampus. *J Neurophysiol* 89: 1414–1422, 2003.

Washburn MS, Moises HC. Inhibitory responses of rat basolateral amygdaloid neurons recorded in vitro. *Neuroscience* 50: 811–830, 1992.

White LE, Price JL. The functional anatomy of limbic status epilepticus in the rat. I. Patterns of ^{14}C-2-deoxyglucose uptake and Fos immunocytochemistry. *J Neurosci* 13: 4787–4809, 1993.

Yamada D, Miyajima M, Ishibashi H, Wada K, Seki K, Sekiguchi M. Adult-like action potential properties and abundant GABAergic synaptic responses in amygdala neurons from newborn marmosets. *J Physiol* 590: 5691–5706, 2012.

Zhang JH, Sato M, Araki T, Tohyama M. Postnatal ontogenesis of neurons containing $GABA_A$ alpha 1 subunit mRNA in the rat forebrain. *Brain Res Mol Brain Res* 16: 193–203, 1992.

Zucker RS, Regehr WG. Short-term synaptic plasticity. *Annu Rev Physiol* 64: 355–405, 2002.